University of Stavanger

Faculty of Science and Technology

MASTER'S THESIS

Study program/ Specialization: Petroleum Engineering/ Drilling	Spring semester, 2014. Open
Writer: Kristian Fredagsvik	…… (Writer's signature)
Faculty supervisor: Rune W. Time	
Thesis title: Use of ultrasonic and acoustic sensors for characterization of liquid-particle flow and evaluation of hole cleaning efficiency	
Credits (ECTS): 30	
Key words: Liquid-particle flow, slurry, ultrasound, ultrasonic, acoustic, hole cleaning	Pages: 83 + enclosure: 18 Stavanger, 16.06.2014.

Use of ultrasonic and acoustic sensors for characterization of liquid-particle flow and evaluation of hole cleaning efficiency

Acknowledgements

I would like to thank Rune W. Time for giving me the opportunity to write this thesis. His guidance and knowledge during this project has been of great help.

A grattitute to my friends and family who have supported me and given me motivation through this year.

A special thanks to Oskar Fredagsvik and Karen Haga Vange for helping me proofread.

Abstract

The transportation of solids by suspension can cause severe damage to pipelines and infrastructures if not handled correctly. An adequate system for monitoring multiphase flow can be used to get early indications of erosion and poor hole cleaning. The use of ultrasonic and acoustic sensors has been reviewed for the application of slurry monitoring and evaluation of hole cleaning.

The theories of slurry flow in pipes are quite extensive and are mostly based on fluid mechanics. The various aspects of liquid-particle flow including flow patterns, pressure drop, particle transport and particles in suspensions have been studied. In order to characterize these flows, several non-intrusive methods such as ultrasonic, acoustic, sonar, nucleonic and electrical capacitance tomography (ECT) shows good accuracy. State-of-art systems in each category with accuracies are collected for comparison. The working principle of each system is described with sufficient theory. Various studies within acoustic and ultrasound, including detection of oversized material, velocity measurements and attenuation measurements, are useful for characterization of complex flows.

Wellbores are extended over longer distances with incline and horizontal sections to increase production and reduce the number of offshore platforms. To reach the pre-determined target in the reservoir, at a given depth and offset, hole cleaning must be considered. The outcome of poor hole cleaning in complex wells, will likely end up in sidetracking and abandoning, both costly operations. In the conventional vertical well, hole cleaning had no large impact compared to the more extensive wells. Hence the field of hole cleaning is now becoming more and more an important tool for hole improvement.

A method is presented in this master's thesis, where hole cleaning efficiency is obtained by measuring drill-cuttings. The system utilize image analysis tool for Particle-Size Distribution (PSD), Cuttings morphology-tool for cuttings morphology, Roman Spectroscopy for cuttings mineralogy and Cuttings flow meter for total weight cuttings. The tool has been tested in the Cubility center in Sandnes and at rigsite. Some alternative methods such as Ultrasonic Flow Meter (USFM) for volume flow and Ultrasound Extinction (USE) to determine PSD are also discussed.

Nomenclature

Roman symbols

A	Cross sectional area [m^2]
A_i	Amplitude level after increasing solid concentration
A_{oi}	Amplitude level before increasing solid concentration
b	$[(i\omega\rho_f/\eta)^{0.25}p_b]$
B	Bulk elastic modulus [Pa]
c	Speed of sound in the medium [m/s]
C	Volumetric concentration
C_{mb}	Concentration of the moving bed
C_s	Solid concentration
d_{50}	Mass-median particle diameter [m]
d_p	Solid particle diameter [m]
D	Pipe inner diameter [m]
D_h	Hydraulic diameter [m]
f	Frequency [Hz]
f_d	Doppler shift [Hz]
f_o	Transmitting frequency [Hz]
F_{hG}	Gravitational force acting on the suspended layer, due to inclination [N]
F_{mb}	Friction forces from particles in the moving bed against the surface of the pipe wall S_{mb} [N]
F_{mbG}	Gravitational forces acting on the moving bed layer [N]
F_{mbsb}	Friction force in the interface between the moving bed and stationary bed S_{mbsb} [N]
k	Ultrasound wavenumber [m^{-1}]

ka	Wavenumber with characteristic dimension of the scattering center
kr	Non-dimensional acoustic wavenumber
K	Fluid consistency index [$Pa \cdot s^{0.07}$]
KRT	Kurtosis
L	Length [m]
M	Number of points in the signal
N	Fluid behavior index
Q	Transport rate [m3/s]
Re	Reynolds Number
S	Interface
S_{PD}	Relative particle density
T	Period [s]
U	Velocity [m/s]
U_{cm}	Critical velocity [m/s]
$U_{convect}$	Phase speed of the disturbance [m/s]
U_{m1}	Flow velocity of layer 1 [m/s]
U_{m2}	Flow velocity of layer 2 [m/s]
U_s	Superficial velocity [m/s]
V	Terminal settling velocity [m/s]
Vol%	Volume percent
Wt%	Mass fraction in percentage by weight
y	Signal value
$\bar{y}$	Signal mean

Greek symbols

α_1	Volumetric concentration layer 1
α_2	Volumetric concentration layer 2
α_c	Contact load
α_{int}	Attenuation due to Intrinsic mechanism
α_P	Total attenuation with three mechanisms
α_{s1}	Solid concentration of layer 1
α_{s2}	Solid concentration of layer 2
α_{sc}	Attenuation due to scattering mechanism
α_{st}	Attenuation due to structural mechanism
α_T	Total attenuation with six mechanisms
α_{th}	Attenuation due to thermal mechanism
α_{vic}	Attenuation due to viscous mechanism
β	Inclination [^{0}]
β_{eff}	Effective compressibility
γ_p	Bed height associated with moving bed [m]
γ_{sb}	Bed height associated with the stationary bed [m]
δ	ρ_f/ρ_s
ΔP	Differential pressure [Pa]
$\Delta\alpha_V$	Correction for large kr in terms of absorption
ε	Pipe roughness
ε_{dc}	Diffusion coefficient
θ_{mb}	Angle associated with the moving bed [^{0}]
θ_{sb}	Angle associated with the stationary bed [^{0}]

λ	Wavelength [1/m]
μ	Viscosity [kg/ms]
μ_L, γ_L	Lame elastic constants of the particles
ρ	Density [kg/m^3]
ρ_{eff}	Effective density [kg/m^3]
ρ_s	Density of solid [kg/m^3]
σ	Signal standard deviation
τ_h	Shear stress on the suspended layer of perimeter S_h [Pa]
τ_{hmb}	Interfacial shear stress between the homogeneous layer and moving bed layer S_{hmb} [Pa]
τ_{hmb}	Shear forces in the interface S_{hmb} [Pa]
τ_{mbsb}	Shear stress acting in the interface S_{mbsb} [Pa]
φ	Solid volume fraction
ω	Temporal frequency [rad/sec]
v	Velocity [m/s]

Abbreviations

AE	Acoustic Emissions
BHA	Bottom Hole Assembly
DNV	Det Norske Veritas
ECD	Equivalent Circulating Density
ES	Electrical Stability
MSM	Mud Solids Monitor
MWD	Measurement While Drilling
PAC	Polyanionic Cellulose
PIV	Particle Image Velocimeter
PRF	Pulse Repitition Frequency
PSD	Particle-Size Distribution
RPM	Revolutions Per Minute
USE	Ultrasound Extinction
USFM	Ultrasonic Flow Meter
UVP	Ultrasonic Velocity Profile
XRF	X-Ray Fluorescence

Terms and Definitions

Apparent Viscosity defines the viscosity of non-Newtonian slurry at the particular rate of shear. The viscosity of a non-Newtonian fluid is dependent on time and magnitude of flow. A single point measurement and assuming constant shear rate is not applicable for non-Newtonian slurries. The continuous deformation causes variations in the viscosity, and a wide range of shear rates are needed to fully understand the behavior of the flow. Most slurry can be expressed by shear rate and shear stress by the form

$$\tau = \eta\dot{\gamma} \tag{1}$$

$$\eta = \frac{\tau}{\dot{\gamma}} \tag{2}$$

where τ is shear stress, η is apparent viscosity and $\dot{\gamma}$ is shear rate. For ideal fluids, also called Newtonian fluids, the shear stress and shear rate contribute to a linear relationship in rheograms. For the non-Newtonian fluids, this relationship is non-linear due to the deformation effects within the liquid. The non-Newtonian liquids can however be categorized as Pseudo-plastic or dilatant. Pseudo-plastic is often referred to as shear thinning and Dilatant is referred to as shear thickening. The three behaviors are seen in the Figure 1 [1,2].

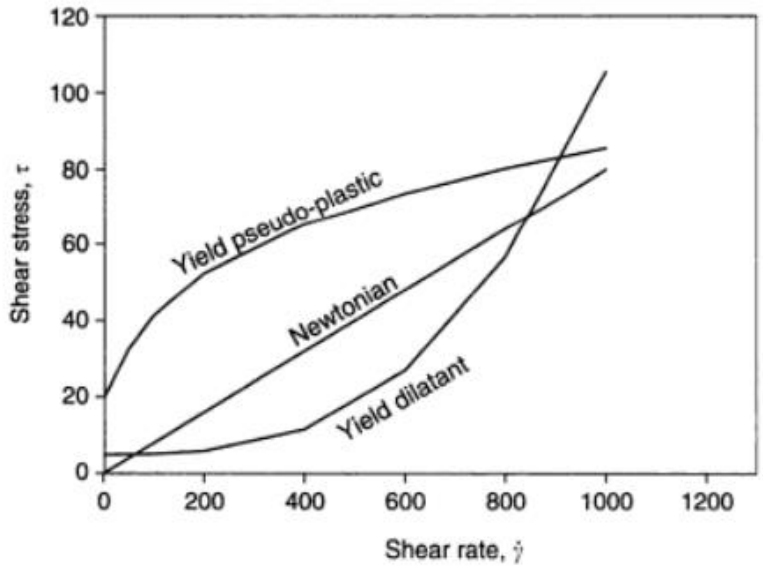

Figure 1: Rheogram including Newtonian and non-Newtonian fluid [1]

Colloids are systems of substances dispersed in another substance with range from 1 nm to 1 µm

Critical velocity describes the flow velocity where particles will go from suspension to accumulating at the bottom of the pipe. This transitional velocity is difficult to determine experimental since flow becomes unstable near transitional velocities [1]

Drag force is the resistance of a particle to motion and depends on the velocity of the body relative to the medium, density, viscosity, cross-sectional area of the pipe and roughness of the surface. The drag force acts in the opposite direction of the velocity and is given by

$$F_D = \frac{C_D A \rho V^2}{2} \tag{3}$$

where C_D is the drag coefficient, A is the cross-sectional area, V is the particle velocity [10]

Grain Reynolds number (Re_g), is defined as the product of the shear velocity (u*) and grain size (d_s) divided by the fluid kinematic viscosity (ν)

$$Re_g = \frac{u^* d_s}{\nu} \tag{4}$$

Sauter mean diameter is defined as the diameter of a sphere that has the same volume/surface area ratio as a particle of interest

Shear forces are the dynamic forces acting on the surface area to deform a particle and is given by

$$F_s = \tau_{xy} S \tag{5}$$

where S is the surface area. The shear forces acts on particles in no-slip conditions. If the fluid and solid velocity are not equal at the interface, there are no shear forces; the fluid slips past the particle. Shear forces occur in fluid layers and solid boundaries where fluid flows by

Slurry density can be expressed as mixture density, ρ_m, given by

$$\rho_m = (\alpha_s \rho_s + (1 - \alpha_s) \cdot \rho_l) \tag{6}$$

Slurry flow velocity is based on volumetric flow rates of solid,$\dot{V}_s$, and liquid, $\dot{V}_l$. The mean velocity is defined by

$$Um = \frac{(\dot{V}_s + \dot{V}_l)}{A} \tag{7}$$

Solid concentration can be expressed by volume fraction α_s or mass fraction

$$\alpha_s = \frac{\dot{V}_s}{(\dot{V}_s + \dot{V}_l)} \tag{8}$$

and the mass fraction, C_s, is given by

$$C_s = \frac{\rho_s \dot{V}_s}{(\rho_s \dot{V}_s + \rho_l \dot{V}_l)} \tag{9}$$

hence

$$C_s = \frac{\alpha_s \rho_s}{(\alpha_s \rho_s + (1 - \alpha_s) \cdot \rho_l)} \tag{10}$$

Turbulent diffusion is the transport of mass, heat, or momentum within a system due to random and chaotic time dependent motions

Contents

Table of Figures

List of Tables

Introduction and Objective

In the Petroleum industry there is a wide area of uncertainties when it comes to real-time measurement of liquid-particle flow. Solid content is often added in the drilling mud to ensure hole stability and proper hole cleaning. Omland et al. (2007) stated in the paper for SPE:

> In field applications, there has been reluctance towards trusting solid control equipment for controlling the particle size distribution (PSD) and particle content of the drilling fluid system, since no real-time monitoring equipment has been available to produce the necessary measurements [51].

In the pipeline industry, such as mining and oil & gas, conveying slurries have been handled for several decades, but the theory including suspended solids in liquid, still remains partly uncertain. As solids are suspended in liquid flow, they tend to cause damage to facilities and need to be monitored. Uncontrolled processes can result in equipment failure, risk to life, environment and property. Hence real-time control of liquid-particle flow is needed for obtaining information on flow dynamics parameters such as particle concentration, flow speed, turbulence intensity and particle size, to fully characterize the multiphase of liquid-particle flow. There are several classification schemes to provide a basis for describing the behavior of solid-liquid mixtures, the two most common are based on physical properties and rheology, or flow behavior [53].

The use of ultrasound measurements is a non-intrusive, environmental friendly, fast response for on-line measurements, and is often cost effective versus alternative methods. The use of ultrasound started already in 1883, when Sir Francis Galton developed the whistle. It was not until 1917 the ultrasound was introduced in terms of technological application when Paul Langevin applied ultrasound to detect submarines. Since then, ultrasound has been used in a wide range of applications within medicine, industry and science. In medicine ultrasound is a basis for cancer treatment, kidney stone treatment, as diagnostic tools and fetus images by 3D ultrasound. Examples of industrial application are thickness measurements, non-destructive testing (NDT), flow speed measurements, fish detection in wells, navigation by sonar, leak detection in casings, tubing and wellheads and confirmation of casing-cement bond. Due to

the wide range where ultrasound can be applied, there are extensive studies ongoing on developing new industrial ultrasonic methods, including methods for liquid-particle flow.

In this master's thesis the objective is to present multiphase flow consisting of liquid-particle in various forms. A literature study of the main theories and impact of this type of flow is part of the scope of this thesis. An effort of finding reliable studies and technology of hole cleaning application with ultrasonic methods is also included. In the industry there is a large number of manufacturers that develops both intrusive and non-intrusive systems for monitoring multiphase flows. To get an overview and map the available non-intrusive systems are also parts of the thesis. By reviewing the different methods that are available, ultrasonic or not, gives a better chance of developing new and improved methods. One of the driving factors is that per day there are no good techniques to fully monitor the hole cleaning efficiency. Some of the questions that should be answered are; can ultrasonic methods be adequate tools for this purpose? Which uncertainties would such a system imply?

1. Theory

1.1 Liquid-Particle Flow

Liquid-particle flow is the suspension of particles in a carrier liquid and is often referred to as slurry. The transport of slurry is widely used in several industries such as mineral, coal, chemical, food and water. The transport relies on higher flow velocity for these multiphase flows in order to keep the particles in suspension. Single phase flow will act as a homogeneous flow independent of flow velocity. Slurry on the other hand may act as heterogeneous depending on the flow velocity [1].

Durand and Condolis (1952) developed a classification of slurry flows based on average particle size in 1952. Since then, other refined classifications have been introduced. The most common classification categorizes liquid-particle in horizontal flow in 4 modes or regimes: Stationary bed, Moving bed, Heterogeneous flow and Homogeneous flow. The four regimes are illustrated in Figure 2 [1].

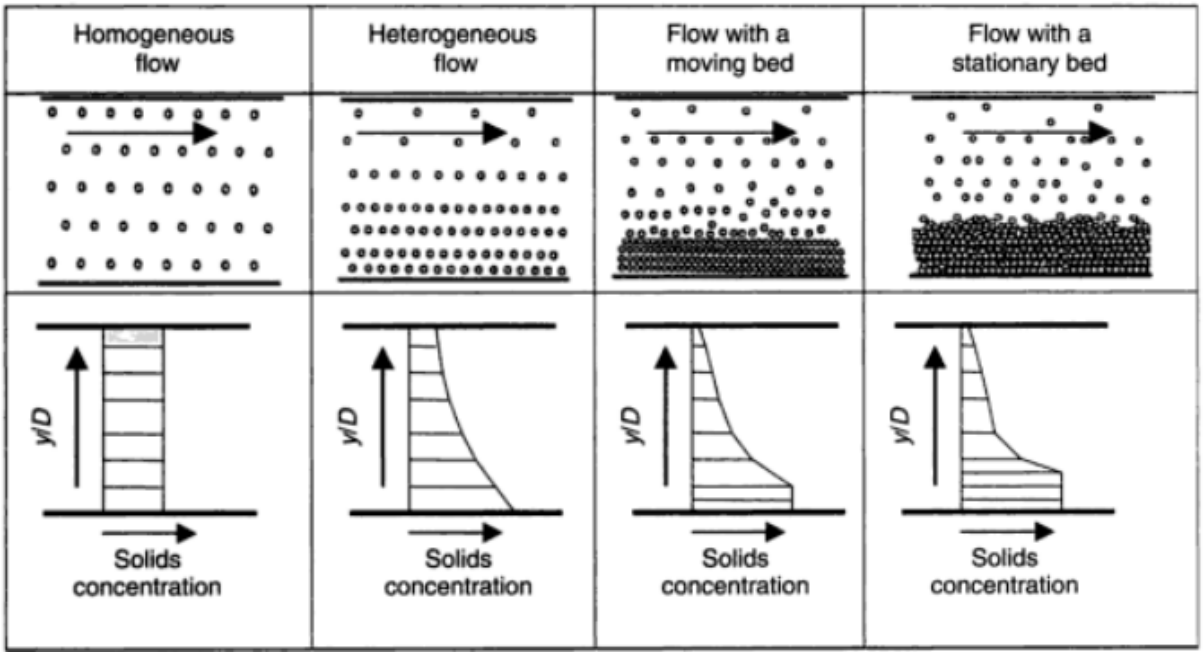

Figure 2: Illustration of particle distribution and solids concentration profile [1]

Stationary beds, illustrated on right side in Figure 2, occur when the slurry velocity is too low to move the particles, resulting in deposition at bottom part of the pipe. The stationary beds

are transported as a separate layer. This type of flow should be avoided since it is highly unstable and can result in worst case scenario which is plugged pipe [1].

Moving beds are a result of increasing mixture velocity compared to stationary beds. Denser particles will slide along the bottom of the pipe. The shear forces exerted from the fluid are sufficiently high enough to move the particles in this flow regime. The upper part of the pipe will act as a heterogeneous mixture [1].

Heterogeneous slurry flows are liquid combined with solid particles and density and size properties sufficient to stay in suspension, but form a non-uniform solid concentration. The solid concentration increases from top of the pipe where lighter particle flows, to the lower side of the pipe dominated by denser particles with higher concentrations. The solid concentration in heterogeneous flows can be as high as 35 wt% and is often present in industry such as mineral processes. Heterogeneous flows are complicated and many experiments and literature are based on this flow pattern. Critical deposit velocity and pressure losses are parameters of interest when studying heterogeneous flows in horizontal pipe. Heterogeneous flow regime in pipes is similar to the suspension transport in rivers [1].

Homogeneous slurry flows are defined as particles in fully suspension with uniform concentration. High concentration of fine particles with low density allows the slurry to act as a single phase flow. Although it will never be completely homogeneous due to its distinct phases, these flows can often be described by single phase models [1]. Homogeneous slurries can have particle concentration as high as 60 wt% and still keep its uniformity. When the solid concentrations increase the viscosity increases and the mixture develop non-Newtonian properties. Typical homogeneous slurries are clays and drilling mud [1].

1.2 Particle Transport

The hydrocarbon industry is exposed to complex multiphase flow, because oil and gas are produced through pipelines. New technology allows extended horizontal wells and subsea production systems, which is a challenge due to unwanted sediments transportation upstream. Understanding the mechanism of particle transport is an important aspect in designing new horizontal wells. When drilling through weak or unconsolidated reservoir rocks, particles and

sand grains will easily detach and be carried with the flow upstream and cause erosion and blockage of flow lines and separators. When sand occupies critical volume in the separator it often results in reduced separation and safety hazards if pipes fail due to sand erosion. Statoil together with Det Norske Veritas (DNV) found that the same amount of sand causes a thousand times more erosion in wells with high flow rates than wells with low flow rate. The ability to predict the particle transport is therefore crucial. A safe limit of two kilograms a day per well, was identified for the Gullfaks field [4].

1.3 Particle Support Mechanism and Suspension of Settling Slurries

Particles in a slurry flow are dependent on gravity forces and density differences in order to stay in suspension. Particles avoid accumulation due to several mechanisms which all act against gravitational forces. One important mechanism is the "turbulent diffusive action of the conveying fluid" [10], which supports the weight of the particles in the flow, either homogeneous or heterogeneous. Inter-particle contact as a result of higher solid concentration, packing of particles and increasing particle-particle interactions will oppose effect against gravity.

Turbulent flow is a complex and irregular flow, but very important regarding transportation of particles in pipes. In the next section turbulence will be reviewed in detail. A simple observation is by turning on a tap, and increasing the flow velocity. As water starts to flow, it is completely transparent. Increasing the flow, the water is now rushing and is more chaotic as flow velocity and pressure varies rapidly. This flow regime is described as turbulent flow. Through the years, numerous people have described and argued on the term called coherent structure. Coherent structures are basically the study of order in disorder within turbulence. Hussain (1981) described the structures as following:

> A coherent structure is a turbulent fluid mass connected by a phase-correlated vorticity. That is, underlying the three-dimensional, random vorticity fluctuations characterizing the turbulence, there must be a coherent vorticity which is instantaneously correlated over the entire fluid mass. This fluid mass is singly-connected and the coherent vorticity must be instantaneously of the same sign in any

plane; thus, a collection of vortices with phase-correlated vorticity is not a coherent structure [11].

The structures are illustrated in Figure 3 and Figure 4. The coherent structures near the wall lead to strong variations of shear stress and cause particles to uplift from beds. *Burst* are cycles consisting of ejection and sweeping and are the two major events responsible for the production of turbulent stresses, again responsible for sediment transportation [13].

Figure 3: Schematic of a vortex pairing process [12]

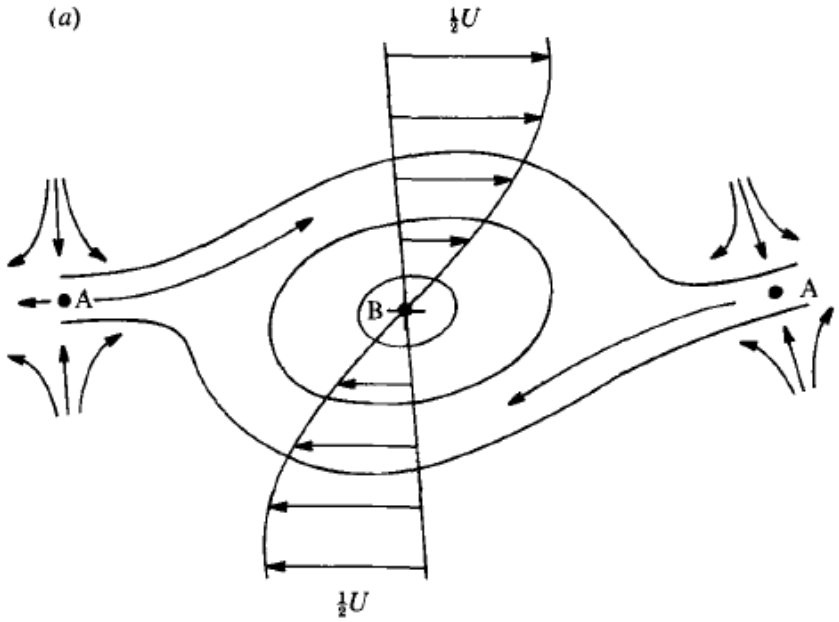

Figure 4: Coherent structure in a plane mixing layer. A is the saddle and B is the center [12]

These turbulent structures can be measured with sonar, and are used to determine volumetric flow rate. The details are explained in *chapter 5.3.1 and 5.8.1*.

In 1851 Georg Gabriel Stokes introduced the Reynolds number (Re), a dimensionless number defined as the ratio of inertial forces (ρ [kg/m^3],U[m/s], L [m]) to viscous forces (μ[Ns/m^2]).

Reynolds number will never fully describe a flow regime, since fluid flow are generally chaotic and small changes as pipe roughness and shape changes can result in a different flow regime. Reynolds number is still very important as guidance of flow regimes and special rules can be applied for non-Newtonian fluid with variable density and viscosity. For flow in pipe the Reynolds number is generally defined as

$$Re = \frac{\rho U D_h}{\mu} \tag{11}$$

where D_h is the hydraulic diameter. The general flow regimes are: Re<2000 laminar flow, when 2300<Re<4000 the flow is in a transition zone, while Re>4000 is defined as turbulent flow. The moody diagram in Figure 5 is very useful to determine the friction factor based on the Reynolds number and relative roughness of the pipe (ε/D).

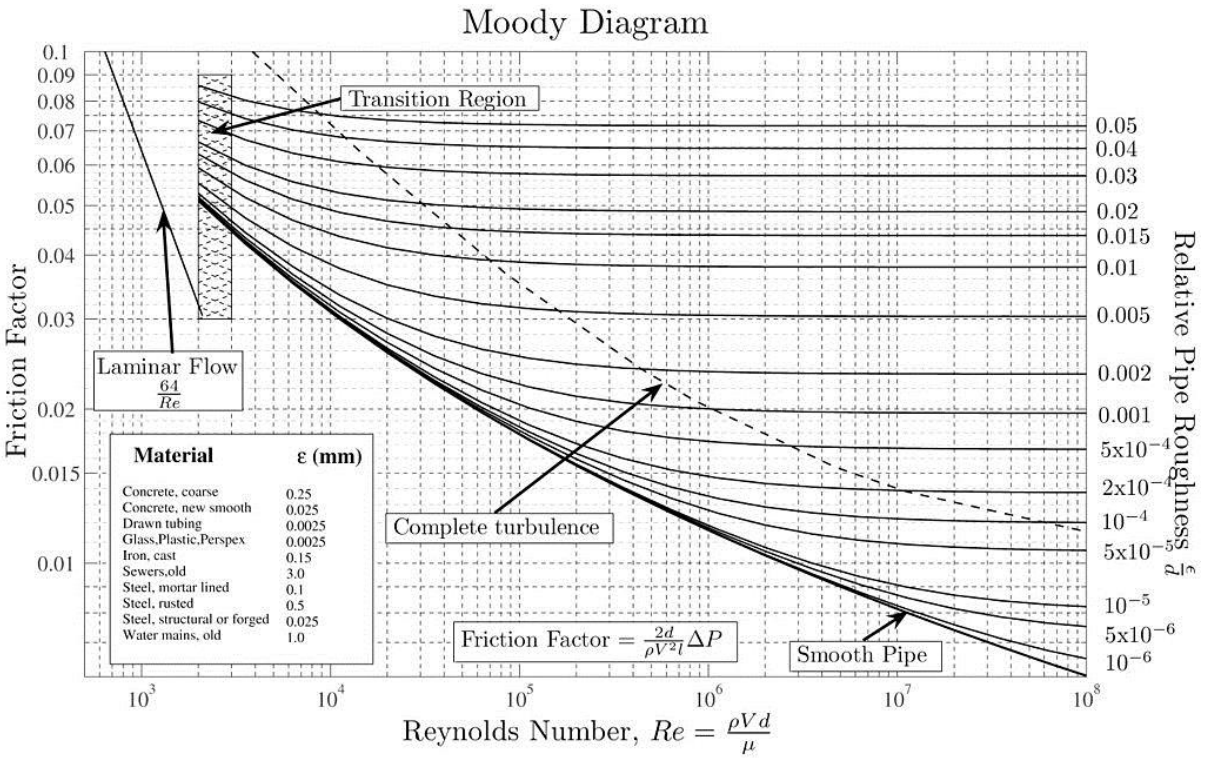

Figure 5: Moody diagram [58]

For non-Newtonian fluids there exist many equations for predicting the friction factor. The correlations are experimental and mostly based on the power law models and assuming smooth pipes such as Dodge and Metzner (1959), Shaver and Merrill (1959), Tomita (1959) Thomas (1960), Kemblowski and Kolodziejski (1973) and Szilas et al. (1981). Figure 6 shows the predicted friction factor using the Dodge and Metzner correlation (1959) [1].

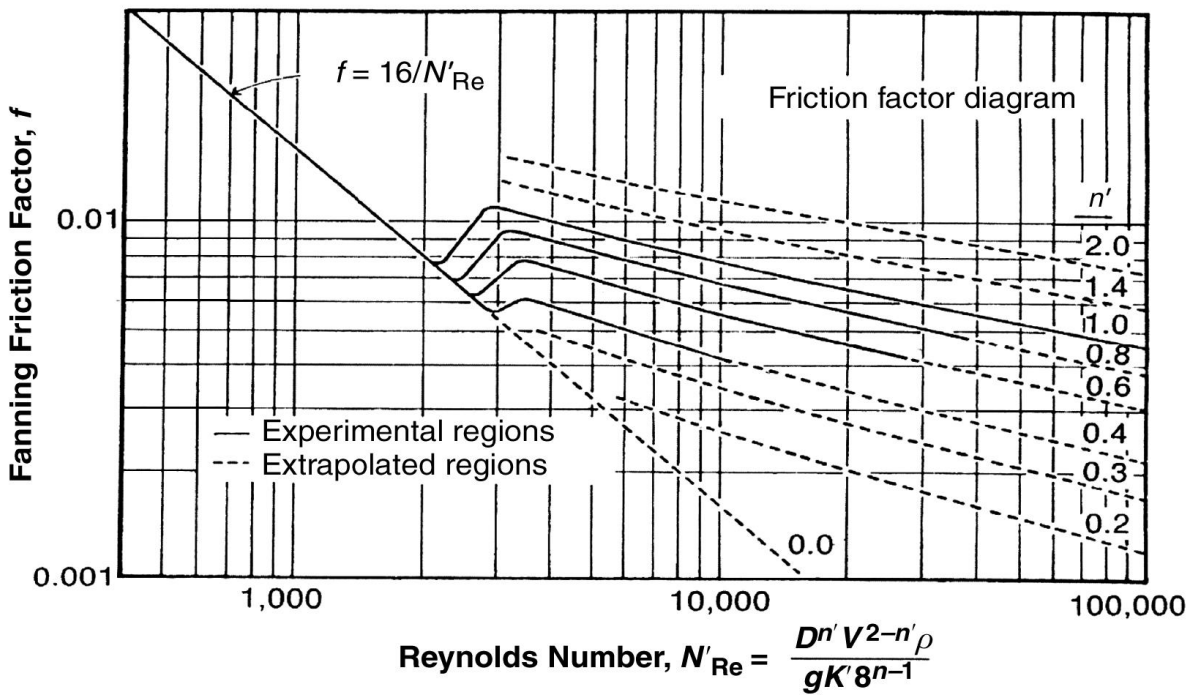

Figure 6: Prediction of friction factor for turbulent flow of pseudo-plastic/power-law slurries in smooth wall pipe using Dodge and Metzner correlation [57]

1.4 Flow Patterns

One important flow pattern in liquid-particle pipeline is the generation of dunes in low and moderate flow velocities. Different dune patterns can be observed as the flow velocity increases and will affect the behavior of the flow. The formation of dunes is a well-known structure found in deserts, rivers, oceans and beaches [1]. The mechanism of moving sand grains forming a dune structure is called saltation. The flow velocity causing saltating beds are higher than flow velocities causing blockage of the pipe, mentioned earlier as stationary bed flow. In the oil and gas industry, cuttings from the drilling operation are transported to surface and are important for wellbore stability. When transporting these cuttings, different bed form will occur and result in flow friction. This will be discussed in chapter *2. Hole Cleaning*.

Rabenjafimanantsoa (2007) [3] discussed and analyzed dune flow for both Newtonian and non-Newtonian water based liquid. A particle concentration of 2 vol% glass beads was used to analyze the relationship between differential pressure ΔP and flow rate. By increasing the flow velocity from 0.14 to 0.72 m/s, the pressure drop was measured and the different flow

regimes were observed. In the first stage the flow velocity were increased to 0.24 m/s and the differential pressure increased as well. In the so-called lower flow regime, no pressure drop variations were noted and only small amplitude dunes were observed. A transition flow regime was observed in the region between 0.24 and 0.46 m/s. In this flow regime, pressure drop was increasing with the increasing velocity, but pressure drop fluctuations at 0.33 m/s of 0.33 mbar were noticed and dune formations were developing and causing unstable flow. The critical velocity is 0.33 m/s and flow with particles in suspension is emerging.

In the last region called upper flow regime, the mixture velocity was increased from 0.46 to 0.72 m/s. The bed form was now antidunes, a stationary bed with saltating particles on top. In Figure 7, the regimes with flow rate and pressure drop are illustrated.

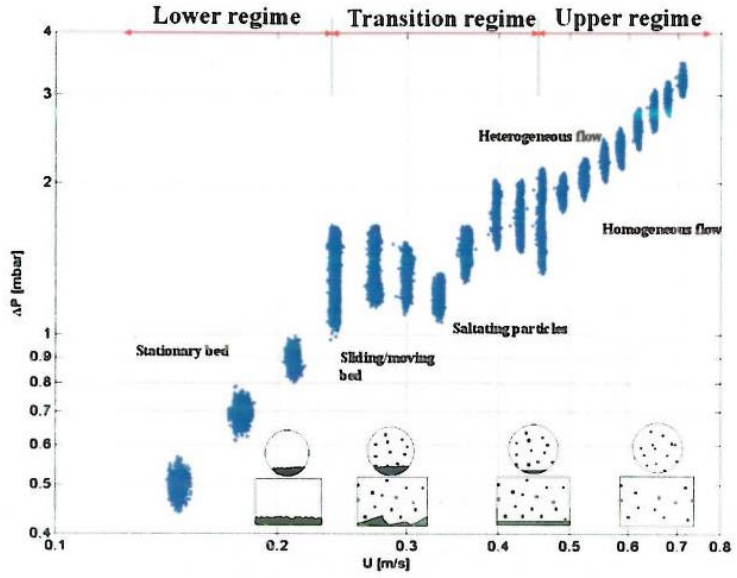

Figure 7: Flow rate and pressure drop [3]

For non-Newtonian experiment, Polyanionic cellulose (PAC) with concentrations of 200 and 400 ppm was used. Rheology and viscosity measurements were taken every 10 seconds. Key observations were that PAC200 and PAC400 had a lower pressure drop in the lower regime than water flow. In the upper regime the PAC's give higher ΔP than water. The flow including PAC may cause the dunes to become more consolidated but less compact than with water as carrier fluid.

The work presented by Rabenjafimanantsoa (2007) [3] showed that formation of dunes had a significant impact on particle slurry transport and the relationship between pressure drop and flow velocity is an important aspect of identifying the different flow regimes.

1.5 Heterogeneous Flow of Settling Slurries from Clayton T. Crowe (2006) [1]

In most industrial transportation systems the liquid-particle flow consist of low particle sizes (~10-20µm) and are treated as pseudo-fluids since the solid particles are uniformly mixed. The systems containing coarse and high-density particles (up to a few millimeters) will not mix uniformly and will settle due to the gravitational effect and are named settling slurries. These types of slurries are categorized in to flow regimes as mentioned earlier: (1) Heterogeneous flow: The high slurry mixture velocity keep the solids suspended by the carrier liquid due to turbulence. (2) Flow with moving bed: At the lower mixed slurry velocity the turbulence is not sufficient to keep all particles in suspension. The accumulated particle at the bottom forms a packed bed of moving particles. (3) Flow with stationary bed: The mixture velocity is too low to transport the accumulated particles and a stationary bed is formed at the lower side of the pipe.

The flow regimes will affect the dependence of pressure drop on the flow velocities as well as pipe erosion and flow performance. The pressure gradient for slurry will always be higher than the pressure gradient for the carrier fluid at same velocities. The differences will expand as the heterogeneity of the mixture increases. This is illustrated in Figure 8 with transitional velocities between regimes.

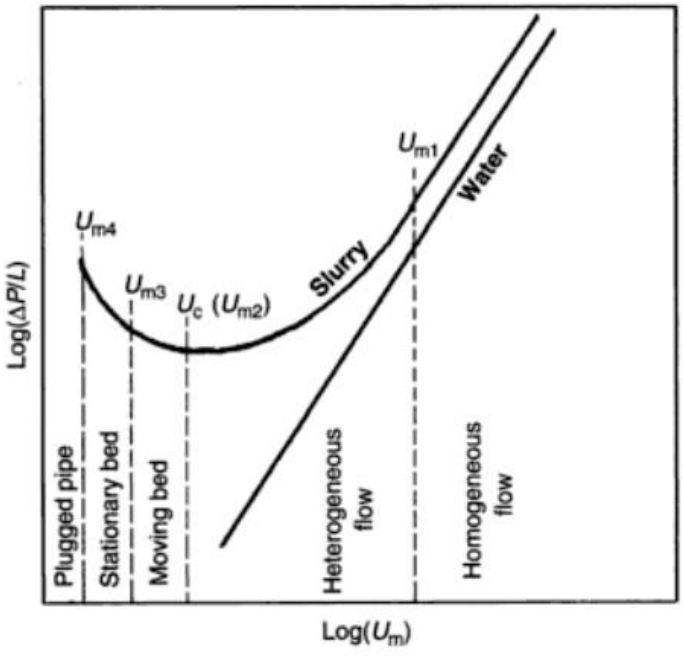

Figure 8: Pressure gradient dependence on mean slurry velocity for flow regimes [1]

As the flow velocity decreases, the pressure drop will also decrease. The point of minimum pressure gradient is often called critical velocity. There are some misconceptions to the term critical velocity, since it often refers to the average velocity required to prevent the accumulation of sediments in the form of moving bed or stationary bed (U_c). The prediction of this velocity is very important in any operation to reduce the risk of pipe blockage. In order to predict this critical velocity several investigations have been done, mostly based on empirical correlations, such as Wilsons Nomogram illustrated in Figure 9 [1].

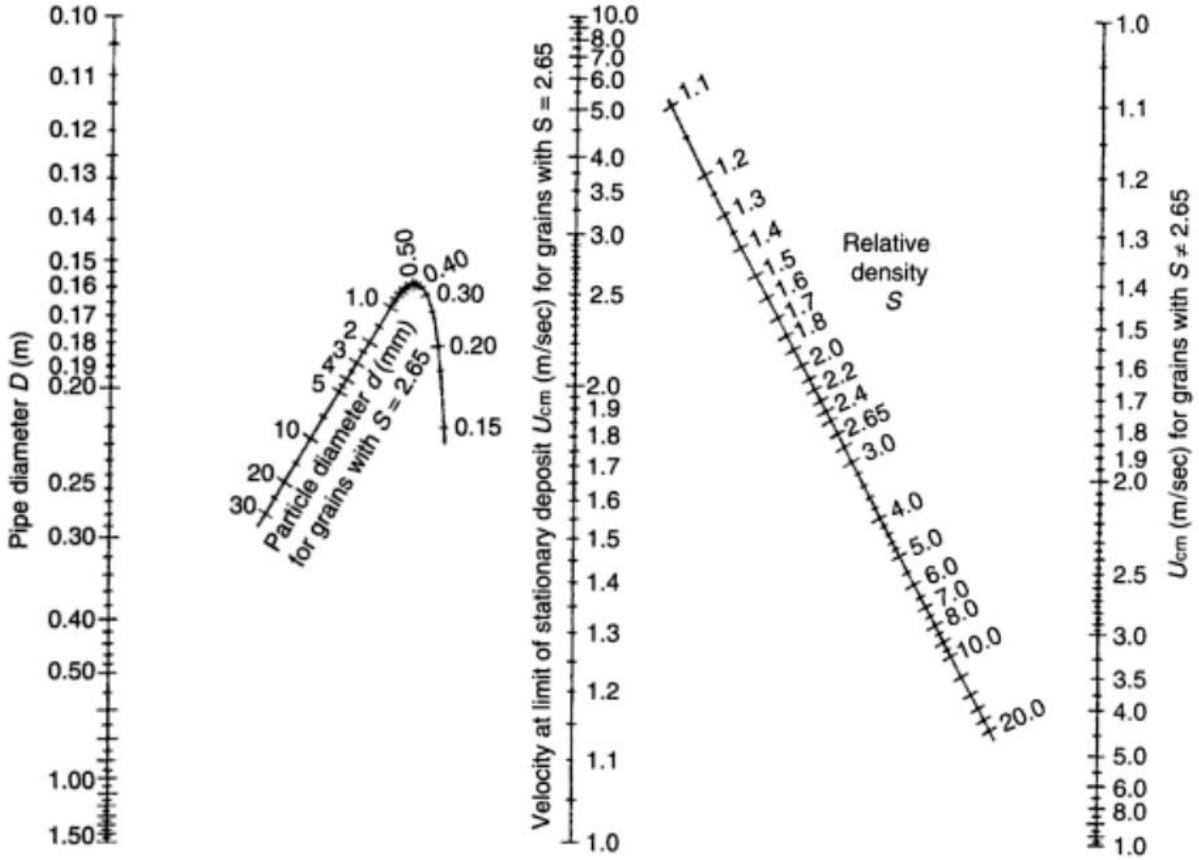

Figure 9: Wilsons Nomogram [1]

The left side of the chart is applicable when the relative weight of the sand ($S_{PD}=\rho_s/\rho_l$) is 2.65. For a given pipe diameter the critical velocity can be determined by drawing a line from pipe diameter through particle diameter (curved line). For particles with relative density not equal to 2.65, a point in the central axis is first determined from pipe diameter and particle density, then this point is joined by a straight line to an appropriate relative particle density, S_{PD}, on the inclined axis. The line will intersect the right hand Critical velocity axis, U_{cm} [1].

1.6 Inclined Pipe of Slurry

The study of conveying slurry in inclined pipe is not comprehensive and rather lacking, although it's very important in several industries. A good experimental setup would require long pipes to achieve a fully developed flow [7]. One important issue regarding inclined pipes is the critical slope. In the design phase of a project it is necessary to determine the critical slope to avoid blockage of pipe in case of a shut down. In case of a shut down, particles will slide down due to the gravitational effect and accumulate in steep bends [1]. Doron, Simkhis and Barnea (1997) [6] stated the critical angle to be 10 to 15% (5-14º). Two models predict flow in inclined slurry flow; "Two layer model" by Shook and Roco (1991) [1] and "Three-layer model" by Doron and Barnea (1996) [5]. The two-layer model is based on the concept of two separate layers, as a hypothetical interface. It is applicable for heterogeneous slurry flow in horizontal and inclined pipes.

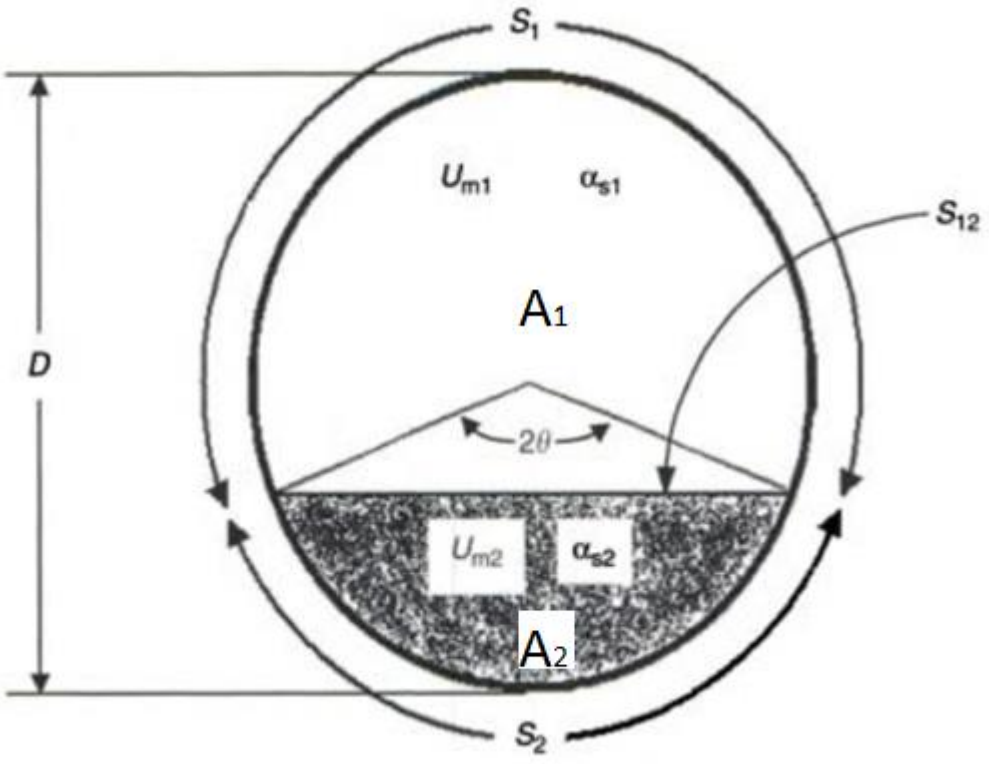

Figure 10: Two-layer model [1]

The model has the following assumptions:

- The upper layer comprises of particles less than 74 µm, while the lower part contains all particle sizes.

- The two layer flows with independent velocities, U_{m1} and U_{m2}. The slip is neglected between layers and uniform volumetric particle concentrations (α_1 and α_2) in each layer.
- Wall shear stress in the upper layer is kinematic (velocity-dependent), while in the lower layer the slurry behaves as a liquid regarding wall shear stress.
- The lower layer is defined as a packed bed with solid concentration (α_{s2}) of 0.6. The upper layer contains solid particle concentration (α_{s1}) in a suspended load. The contact load (α_c) is defined as $\alpha_c = \frac{(\alpha_{s2}-\alpha_{s1})\cdot A_2}{A}$.
- The Coulombic friction force is included for particles in the lower layer against the pipe wall.

The cross sectional area is the sum of A_1 and A_2 is given by

$$A_1 = 0.25D^2(\pi - \theta - sin\theta cos\theta) \quad (12)$$

$$A_2 = 0.25D^2(\theta - sin\theta cos\theta) \quad (13)$$

S_1, S_2 and S_{12} are perimeters in terms of the half angle θ and are defined as

$$S_1 = D(\pi - \theta) \quad (14)$$

$$S_2 = D\theta \quad (15)$$

$$S_{12} = Dsin\theta \quad (16)$$

The model is based on mass balance, force balance and momentum equations (in terms of boundary and interfacial stresses). The mass balance for mixture of solids and liquid is given by

$$U_m A = U_{m1}A_1 + U_{m2}A_2 \quad (17)$$

Clayton concludes that the existence of two separate layers is only for modeling purposes, and should not be implied as physical reality.

The three-layer model was later developed on the basis of the two-layer model and is primary based on experimental studies and more analysis. The horizontal flow in this model consists of three layers occupying the pipe. A stationary bed is formed at the bottom of the pipe with

moving bed of particles above. The upper layer is a homogeneous mixture. Figure 11 below is taken from Doron et al. (1997) and illustrates the theory of a three-layer flow in an inclined duct.

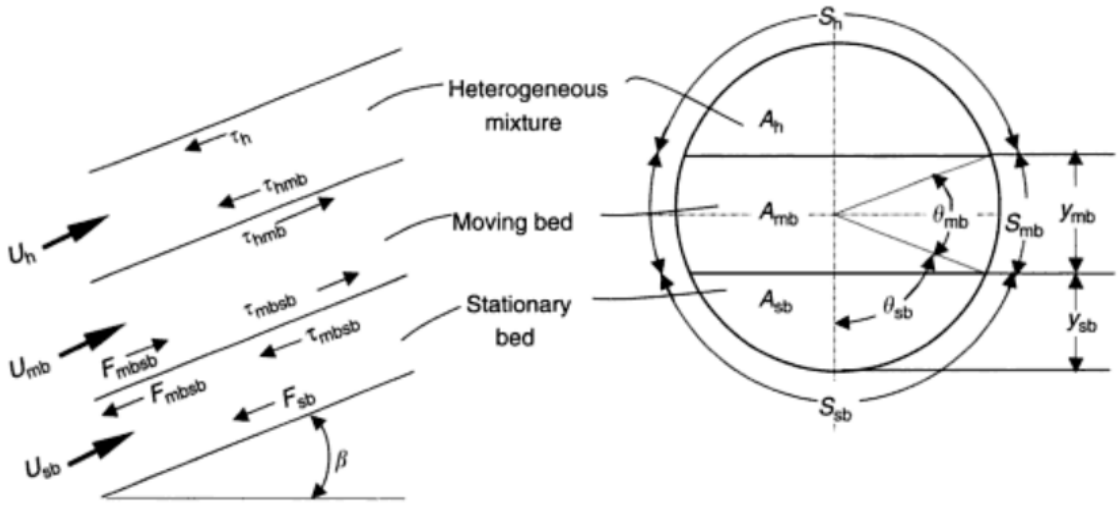

Figure 11: Three-layer model [1]

The model is applicable for horizontal and slightly inclined pipes under conditions with flow rates with three distinct layers of constant thickness and uniform velocities. six equations and six unknown parameters was described by Doron et al. (1997) and will be described here as well.

- U_h: Average velocity of the upper suspended layer.
- U_{mb}: Average velocity of the sandwiched dispersed layer.
- C_h: Average concentration of the upper layer.
- y_{mb}: Height of moving bed.
- y_{sb}: Height of stationary bed.
- dp/dx: Pressure gradient.

For inclined pipes, the minimal bed velocity is a result of forces exerted from the moving particles on the stationary particles including drag and buoyance weight. The forces in this interface must balance and are given by

$$U_{bc} = \frac{\sqrt{1.559(\rho_s - \rho_l) g d_p \left[\sin\left(\frac{\pi}{6} + \beta\right) + \frac{cos\beta}{2} C_{mb}\left(\frac{y_{mb}}{d_p} - 1\right)\right]}}{\rho_l C_d} \quad (18)$$

where β is the inclination of the pipe, C_{mb} is the moving bed concentration and d_p is the solid particle diameter.

Further the continuity equation for solid particle and liquid phase is given respectively

$$U_h C_h A_h + U_{mb} C_{mb} A_{mb} = U_s C_s A \tag{19}$$

$$U_h (1 - C_h) A_h + U_{mb} (1 - C_{mb}) A_{mb} = U_s (1 - C_s) A \tag{20}$$

where A is the cross-sectional area, U_s is the superficial velocity and C is the volumetric concentration. The subscripts h, mb and s refers to homogeneous layer, moving bed and delivered mixture.

By implying pseudo-liquid properties to the upper homogeneous layer, the force balance is written as

$$A_h \frac{dp}{dx} = -\tau_h S_h - \tau_{mb} S_{hmb} - F_{hG} \tag{21}$$

where τ_h is the shear stress on the suspended layer of perimeter S_h and τ_{hmb} is the interfacial shear stress between the homogeneous layer and moving bed layer S_{hmb}. F_{hG} is the gravitational force acting on the suspended layer, due to inclination.

For the moving bed layer the force balance is given by

$$A_{mb} \frac{dp}{dx} = -F_{mbsb} - \tau_{mbsb} S_{mbsb} - F_{mb} - \tau_{mb} S_{mb} - \tau_{hmb} S_{hmb} - F_{mbG} \tag{22}$$

where F_{mbsb} is friction force in the interface between the moving bed and stationary bed, S_{mbsb} and τ_{mbsb} is the shear stress acting in the interface S_{mbsb}. F_{mb} is friction forces from particles in the moving bed against the surface of the pipe wall, S_{mb}. τ_{hmb} is shear forces in the interface S_{hmb}. F_{mbG} is gravitational forces acting on the moving bed layer.

The upper layer is governed by the diffusion equation and by integrating over the upper cross section the mean concentration can be determined by

$$\frac{C_h}{C_{mb}} = \frac{D^2}{2A_h}\int_{\theta_{sb}\theta_{mb}}^{\frac{\pi}{2}} e^{-\frac{DV_s\cos\beta}{2\varepsilon_{dc}}(\sin\gamma-\sin(\theta_{sb}+\theta_{mb}))}\cos^2\gamma\, d\gamma \tag{23}$$

where D is the diameter of the pipe, V is the terminal settling velocity of the solid particles, ε_{dc} is the diffusion coefficient, θ_{sb} is the angle associated with the stationary bed and θ_{mb} is the angle associated with the moving bed.

The six equations are useful for determining transition of flow patterns; for low flow rates the height of stationary beds and moving beds is a part of the model equations. As the flow rate is increased, the transition between stationary bed and moving bed can be determined as the γ_{sb} approaches zero. The limit deposit velocity is associated with the diminishing of stationary bed height. As the flow is further increased and the moving bed height approaches the particle diameter, the transition to fully suspended flow can be determined [7].

Doron et al. (1997) [6] experiments on the effects of inclined pipes, showed that gravitational forces is the governing effect on pressure drop independent on flow pattern. The delivered concentration is estimated to 20%. Another important result is that the stationary bed range was increased as the pipe was tilted upwards and can be seen in Figure 12. The density is 1240 kg/m^3, particle diameter is 3 mm, pipe diameter is 51 mm and solid concentration is 13%.

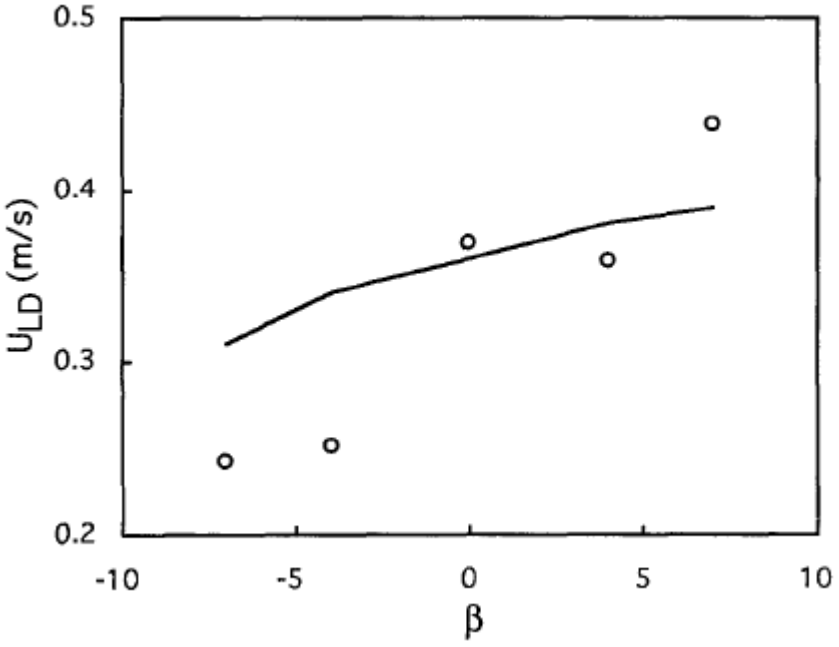

Figure 12: Effect of inclination on limit deposition velocities [6]

The negative effect of bed height in inclined pipes is also illustrated in Figure 13. β is the inclination in terms of degrees. The operation parameters used; ρ_s= 2475 kg/m3, d_p=0.66 mm, D=51 mm, Us=1.3 m/s and C_s=5.8%.

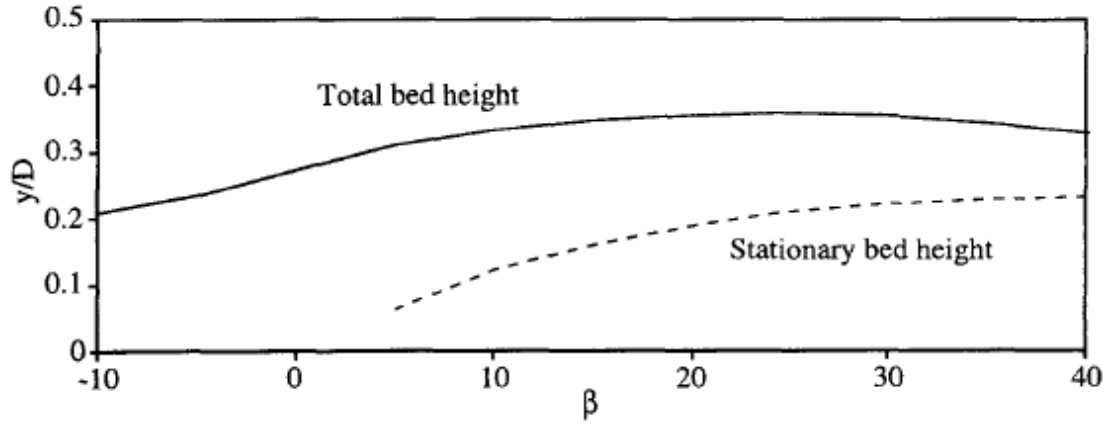

Figure 13: Effect of inclination on predicted bed height [6]

For negative inclinations in Figure 13, the bed heights are at minimum, which induce a positive effect. By increasing the angle to positive values, maximum bed height is reached. The increase in bed height is severely dependent on the change of gravitational force as the pipe is tilted upwards. As the inclination is further increased (>25º) the bed height will decrease.

1.7 Measured Flow Characteristics after Albion et al. (2011) [2]

By measuring different properties of a fluid/slurry in flow in pipelines, a better image of the behavior can be achieved. The knowledge of flow behavior can prevent problems from occurring during the transportation. Several flow regime maps and models are available, but they are based on specific slurry material and pipe diameter and are often not applicable for complex flows such as petroleum related processes. These flows include gas-oil-water flows and can exert pressures of 300 bar and temperatures of 250˚C [1]. In these cases, it is important to monitor pipe flow instead of using charts, so that risk of damage, blockage and inefficient operations is avoided. Downtime is a very serious problem for offshore platforms since they rely on constant production to maintain maximum economic profit. The day rates, depending on the size of the platform can easily exceed 5 to 7 million NOK per day. To stay operational and prevent shutdowns is crucial. Many techniques have been developed to measure slurry flow through pipe, both intrusive and non-intrusive. The following properties of slurry should be measured and monitored:

- Pressure drop: provides details of system operation that can be correlated to determine concentrations, flow patterns and flow velocity.
- Particle and slurry velocity: Determines if the system as it should, by avoiding particle settling causing pipe blockage and erosion. Average velocity and point velocity can be measured.
- Solid concentrations: Either as weight or volume percentage in order to determine if the transport is operating under the reasonable concentrations. Can also indicate problems as pipe blocking and upstream particle feeding problems.
- Flow pattern: Observe that the flow pattern is sufficient to transport particles without causing blockage. Too high flow velocity can result in erosion and pipe failure. The right flow pattern therefore important for effective slurry handling.
- Mass and volumetric flow rates: Determines the slurry velocity in order to ensure that the right operational conditions are kept.
- Presence of foreign object such as large sediments from an unconsolidated reservoir that can cause damage to pumps etc [2].

1.7.1 Pressure drop measurements

As slurry travels through pipelines, several forces are acting on the particles by the fluid. Either as the fluid move around the particle or by velocity fluctuations due to turbulence. The turbulent eddies are constantly lifting particles from the established beds. The suspended particles are affecting the turbulence as they collide with the wall and accelerated by the flow again. Hence the loss of energy from the collision has a direct effect on the eddies.

By correlating pressure gradient with velocity, the flow regime between moving bed and fully suspended flow can be determined (in horizontal flows). At the point of velocity where the pressure gradient is at minimum, indicates the point of transition. As the particles goes from bed to suspension, the pressure gradient increases with velocity.

The various flow patterns rising in pipelines results in different frictional forces. As mentioned earlier, a stationary bed exerts significant friction both viscous and mechanical, causing a pressure drop. From pressure drop measurements, the degree of stratification and amount of particle settlement can be determined, since the flow patterns with beds will cause higher friction than slurry flow with fully suspended particles.

Matousek (2002) [14] did many experiments on the effect of fine and coarse sand particles to frictional pressure drop in different flow patterns. By using a 150 mm pipe in a 24 m long test loop fine sand (d_{50}=0.12), medium sand (d_{50}=0.37) and coarse sand (d_{50}=1.85) was transported in different velocities. Figure 14 illustrates the loop used in the study.

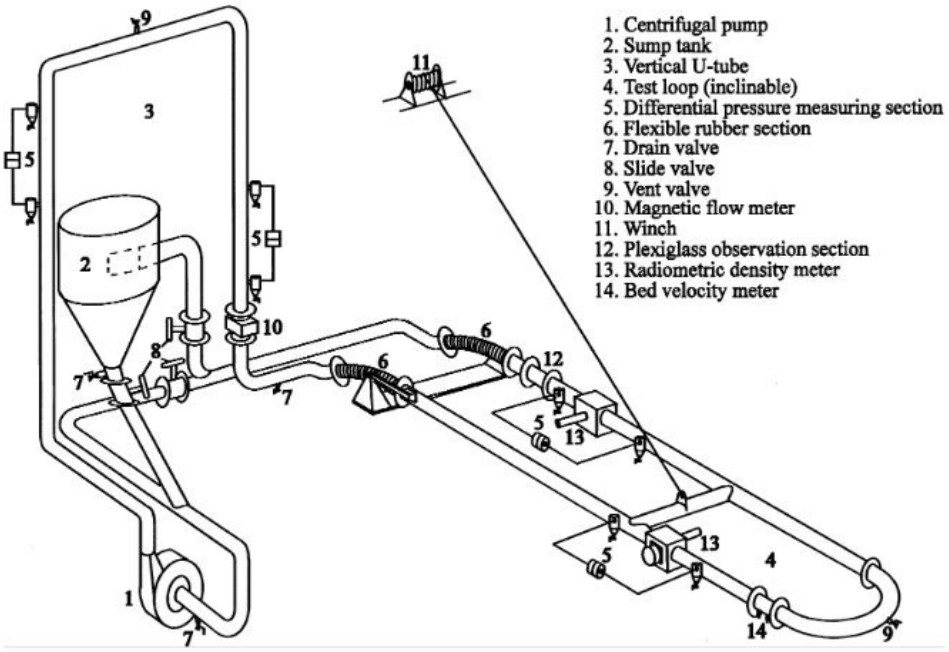

Figure 14: Experimental setup by Matousek (2002) [14]

As expected; at velocities higher than the critical deposition velocity, all fine particle act as suspended flow. The medium coarse sand flow is partially stratified at velocities slightly above critical deposition velocity and suspended at higher velocities. By comparing the pressure drop of flow with fine sand and medium coarse sand in the range of 1 to 4 m/s, it is noted that flow with fine sand gives less frictional pressure drop than the coarser sand. The coarser sand flow is more sensitive to increase in concentration in the terms of frictional pressure drop. The flow with coarse sand shows fully stratification at a broad range of velocities, and the frictional pressure drop is higher than both medium coarse and fine sand. When increasing the concentration, the coarse sand flow did not increase in frictional pressure drop [14].

1.7.2 Velocity measurements

Flow meters are commonly used to measure flow rate and superficial velocity [1]. In industrial pipelines, 95% of these operate under turbulent flow and flow meters should therefore be designed to work under these conditions.

Some of the velocity measurements methods that will be reviewed are Transit Time (TT) Ultrasonic Flow Meter, Ultrasonic Doppler Flow Meter (USFM), Particle Image Velocimeter (PIV) and Ultrasonic Velocity Profiling (UVP).

2. Hole Cleaning

Vertical wells were the most common wells until recent years. The more complex inclined and horizontal well, has an impact on hole cleaning. In this chapter, the basics of solid transportation in terms of hole cleaning, are reviewed. An effort to reveal ultrasonic and acoustic measurements for monitoring cuttings has been done.

2.1 Cuttings Transport in Horizontal and Inclined Wells

Cuttings are transported to the surface by circulating drilling mud through the annulus between the drill pipe and the open borehole. Cutting size is an important factor for the transportation. Larger cutting relies on high fluid flow rate while smaller cuttings (0.45-3.3 mm) depend mostly on pipe rotation and rheology [8]. Vertical well are in general easier in a hole cleaning perspective, since the detached rocks fall in opposite direction to the mud flow. In the inclined wells the flow velocity has horizontal component, and hence a reduced vertical component. Suspension of particles in inclined well are therefore more challenging compared to vertical wells. As the inclination increase, the distance for cuttings to fall to the wellbore wall is less. Once the particle slips through the mud and settles, it reduces the chance of transportation due to lower velocity near the wellbore [9]. Insufficient hole cleaning may often result in stuck drill pipe. The stuck drill pipe scenario is a very serious case and can account for half of the total well cost. It is the most expensive problem that can occur during the drilling operation. A mechanical stuck pipe is defined as when the drill pipe is not able to reciprocate or/and rotate and can only be pulled out by damaging the drill pipe without exceeding the maximum hook load of the drilling rig [10].

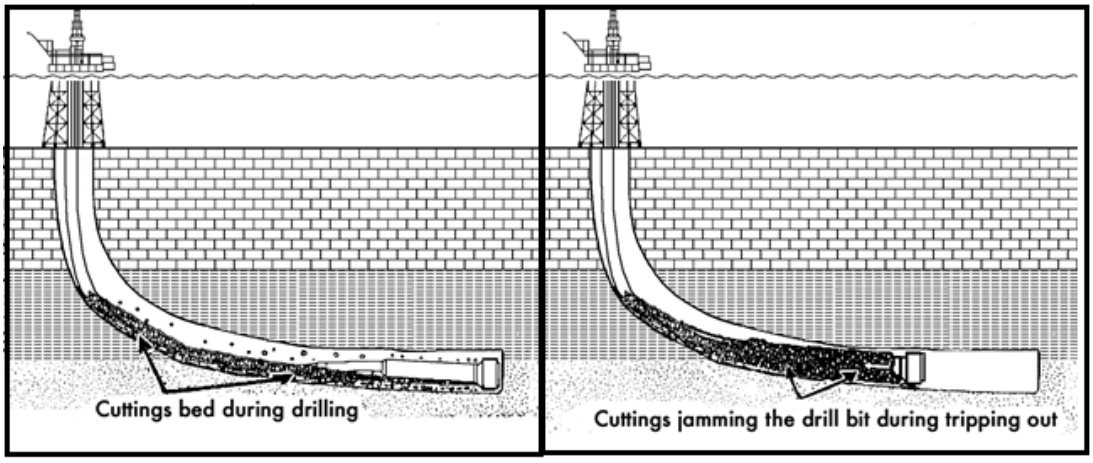

Figure 15: Stuck pipe due to poor hole cleaning [7]

As seen from Figure 15, the cuttings are accumulating near the slope and jam the pipe from tripping up. When comparing vertical wells to inclined well, the flow in inclined well are not annular due to the accumulation of cutting beds on the bottom side of the wellbore. Borehole configuration is defined by cutting bed height, eccentricity of drill pipe and diameter of the open hole and pipe [10]. Ramadan et al. (2005) [7] described the three most common borehole geometrics with an illustration (Figure 16).

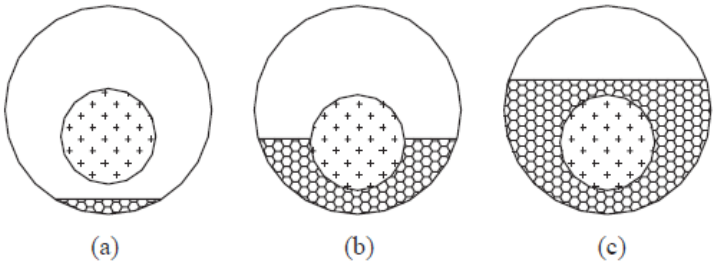

Figure 16: Typical borehole configuration in inclined wells [7]

For inclined wells, the cuttings will accumulate on the low side of the borehole, as seen in Figure 16.

When drilling the well, non-Newtonian fluids such as Bentonite and oil-based muds are often used as drilling fluids. PAC are used for aqueous solutions if oil based muds are not applicable. The non-Newtonian fluids that are used have properties as shear-thinning. These fluids have higher cutting transport ability and optimal frictional pressure loss. In field operations, the yield stress, consistency index and power law exponent are constantly controlled on the surface with the pump rate. Ramadan et al. (2005) [7] mentions in their study that commercially hydraulic and cutting transport models are used to predict the effects of drilling fluid properties and other drilling parameters, but the models need to be modified to minimize hydraulic and cutting transport related problems. A good model for non-Newtonian fluid is required for predicting the cutting transport. The two-and-three layer model by Doran and Barnea (1995) [5] was discussed by Ramadan et al. (2005) and was used as a basis for further analysis. The three-layer model is limited for Newtonian fluid only in horizontal ducts and small inclinations. In order to make the model applicable for non-Newtonian fluid, the slip-ratio needs to be accounted for, since it is neglected in earlier models. The model is described with the following assumptions:

(i) Distinct imaginary interface lines are to exist between the dispersed layer and suspended layer, and between the dispersed layer and the bed.

(ii) Uniform layers are present without significant variation in concentration and thickness along the length of the channel.

(iii) The relative velocity between the particles and the fluid is negligible in the bed.

(iv) The flow is steady and turbulent.

(v) Bed shear stress variation in the lateral direction is negligible.

(vi) Stratified and well-compacted bed to resist the applied shear [9].

The experimental setup is shown in Figure 17 and a more specific description can be further studied in Ramadan et al. (2001) [57]. The overhead tank ensured constant pressure, the hydroclone separates the solids and a control mechanism is used to maintain constant flow rate in the loop during the runs. A flow meter and differential pressure transmitter was connected to a computer to get on-line measurements. Water and PAC solutions were used as carrier fluid and the rheology of the PAC solution was measured before every test and maintained at K=0.050 $Pa{\cdot}s^{0.07}$ (Fluid consistency index) and n=0.7 (Fluid behavior index). The temperature was constant at 20ºC.

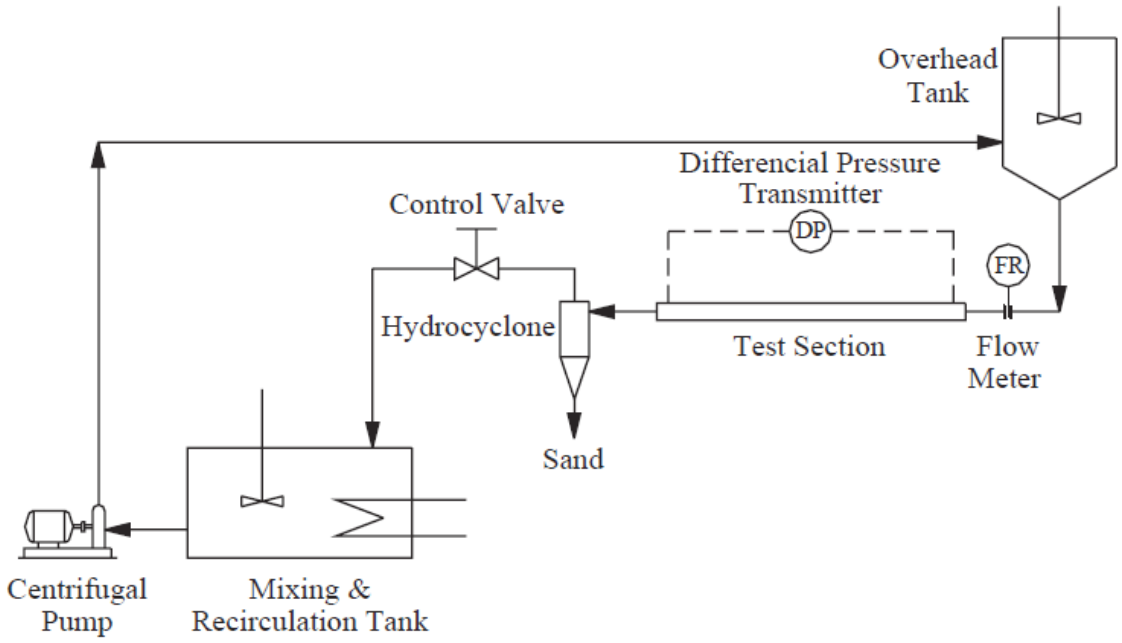

Figure 17: Illustration of flow loop by Ramadan (2001). The test section was 4 m long and internal diameter was 70 mm [7],[57]

Four different particle sizes (0.125–5.5 mm) were used and the condition was set to cover stationary beds at different flow rates. The transport rate [m^3/s] increases with increasing flow

rate, as expected. When the flow rate reaches the critical flow rate, the model prediction becomes inadequate for smaller particle sizes (<1.2 mm). Dunes and ripples occurred when fine sand was tested. According to Ramadan et al. (2005), the formation of these bed forms is dependent on difference between critical velocity and average flow velocity, and the particle size. The probability of dunes and ripples increase as the difference in flow rate arises. The dunes and ripples impose an effect on the cutting transport as mentioned earlier by Rabenjafimanantsoa (2007) in chapter *1.4 Flow Patterns*. The results proves that the three-layer model fails to predict the transport rate near the critical flow rate since the assumption of uniform bed thickness are used [7].

The angle of inclination was increased and the effect of particle size on the transportation rate was studied. By increasing the flow of PAC solution and water, the influence of particle size is significant at high flow rates and low inclinations. The coarse sand beds shows higher transportation rate than the finer sand bed. The cuttings transport with water as carrier fluid is more sensitive to particle sizes [7].

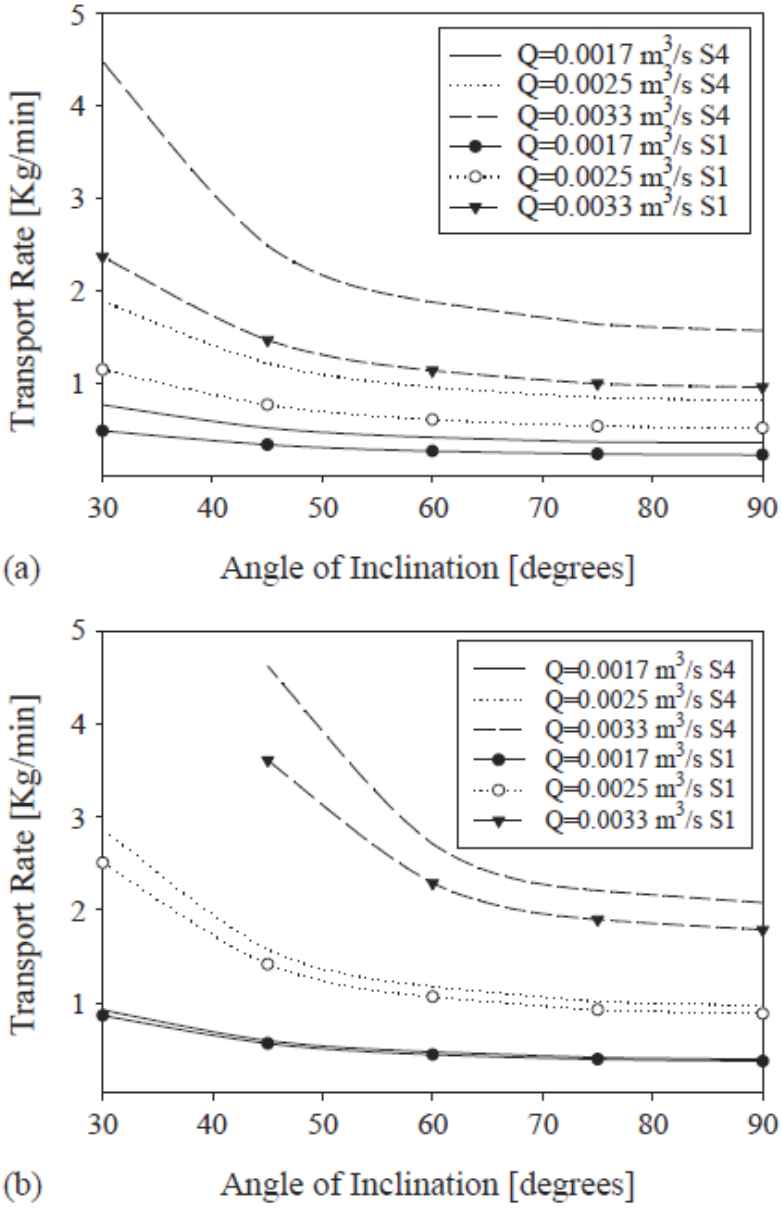

Figure 18: Transport rate vs inclination for (a) water and (b) PAC solution [7]

Figure 18a and Figure 18b shows the effect of particle size on the transportation rate at various inclinations for water and PAC respectively. Fine sand beds are referred to as S1 and coarse sand beds are referred to as S4. The shear thinning PAC solution exerts more viscous then water at higher shear rates. The drag force is higher and particle settling velocity is reduced compared to water. The result is more effective cutting transportation with the PAC solution [7].

Ramadan et al. (2005) concluded that the application of this modified three-layer model, based on experiments and model predictions, are applicable for predicting transport rate of

stationary beds for both Newtonian and power-law fluids. The restrictions of the model occur when critical flow rate and the grain Reynolds number (Re_g) is between 15 and 400 [7].

2.2 MWD Tool for Cuttings Monitoring

Baker Hughes developed a drilling system with sensors for determining properties of drilling fluid down hole. A drill string or coiled tubing provides the drilling assembly to the target depth. The bottom hole assembly (BHA) are equipped with measurement while drilling (MWD) sensors to obtain parameters such as density, viscosity, flow rate, pressure and temperature. The drill bit is driven by rotating the tubing or by a mud motor situated in the BHA. Inside the tubing a drilling fluid is supplied under pressure from the surface and drives the mud motor under drilling operation. The drilling fluid exists at the bottom of the drill bit and returns to surface via the annulus. The returning fluid carries the rock fragments referred to as cuttings. In order to drill successful to target depth within the given time frame, the performance of drilling fluids is a major component in the drilling operation. In scenarios such as deep wellbores and horizontal wells, including harsh environments with high temperatures and pressures, the drilling fluid needs to be designed to perform in several performance categories. The drilling operator and mud engineer determine the type of drilling fluid that is most suitable for the given well. By applying additives the fluid can be designed to have different properties such as:

- Viscosity
- Density
- Gelation
- Mechanical stability
- Chemical stability
- Lubricating properties
- Ability to carry rock fragments to surface and hold cuttings in suspension even when circulation is stopped
- Prevent reactions with rock formations (such as shale swelling caused by water)
- Non-corrosive effect on pipes and drilling equipment
- Provide enough hydrostatic pressure to prevent a kick

- Cooling effect on drill bit [36]

Wellbore stability is commonly dependent on calculating and controlling the density at surface. By applying knowledge of similar operations and information such as rock mechanics, formation dip, formation type and fluid velocity, the fluid density can be determined thereafter. Conventionally the fluid properties are measured by taking samples from the returning well fluid and sending the samples to a laboratory. Even when measuring the properties of the fluid in the lab, the values may be different from the actual value. Near the bit, several thousand meters below the surface, the temperature and pressure are changing constantly and are very different from the surface. Density measurements in conventional drilling that are not real-time, can often differentiate from the density that is needed or assumed. The system designed by Baker Hughes, describes drilling apparatus and methods for determining the fluid density during the drilling operation as well as in-situ measurements of compressibility, rheology, viscosity and solid content [36].

A set of sensors are along the drill string provides measurements of the pressure gradient, temperature gradient and flow rate in the wellbore. Monitoring of pressure gradient and differential pressure of the drill string and annulus will give indications of kicks and accumulation of cuttings [36].

In order to monitor the hole cleaning efficiency, a number of down hole sensors are set for indicating excessive cuttings present in locations along the borehole. In order to transport the rock fragments to the surface, the annular velocity needs to be greater than the slip velocity. The viscosity is based on the size, shape and weight of the cuttings in order to control the settling of particles during operation. A fluid with low shear rate viscosity will keep good carrying capacity in the drilling fluid and density has a buoyancy effect on the transporting cuttings. In general an increase in density of the carrier fluid will act positive on the cutting transportation [36].

The MWD tool described by Baker Hughes is different from other MWD tools, where only parameters related to the formations and physical condition of the tool and the borehole are monitored. By measuring the properties of the drilling fluid during drilling, the operator can faster and easier do corrective actions when needed. The parameters from down hole measurements are computed by a down hole computer or a processor at the surface. The

driller will then be alarmed if unsafe conditions occur, such as gas zone and excessive accumulation of cuttings. A two-way telemetry system connects the surface computer with the down hole processor [36].

The outline of the MWD tool can be seen in Figure 19, with an ultrasonic sensor system. The system will be able to determine cuttings in annulus as well as borehole size. The description of the tool is quite complex and in the next section the system will be explained as simply as possible.

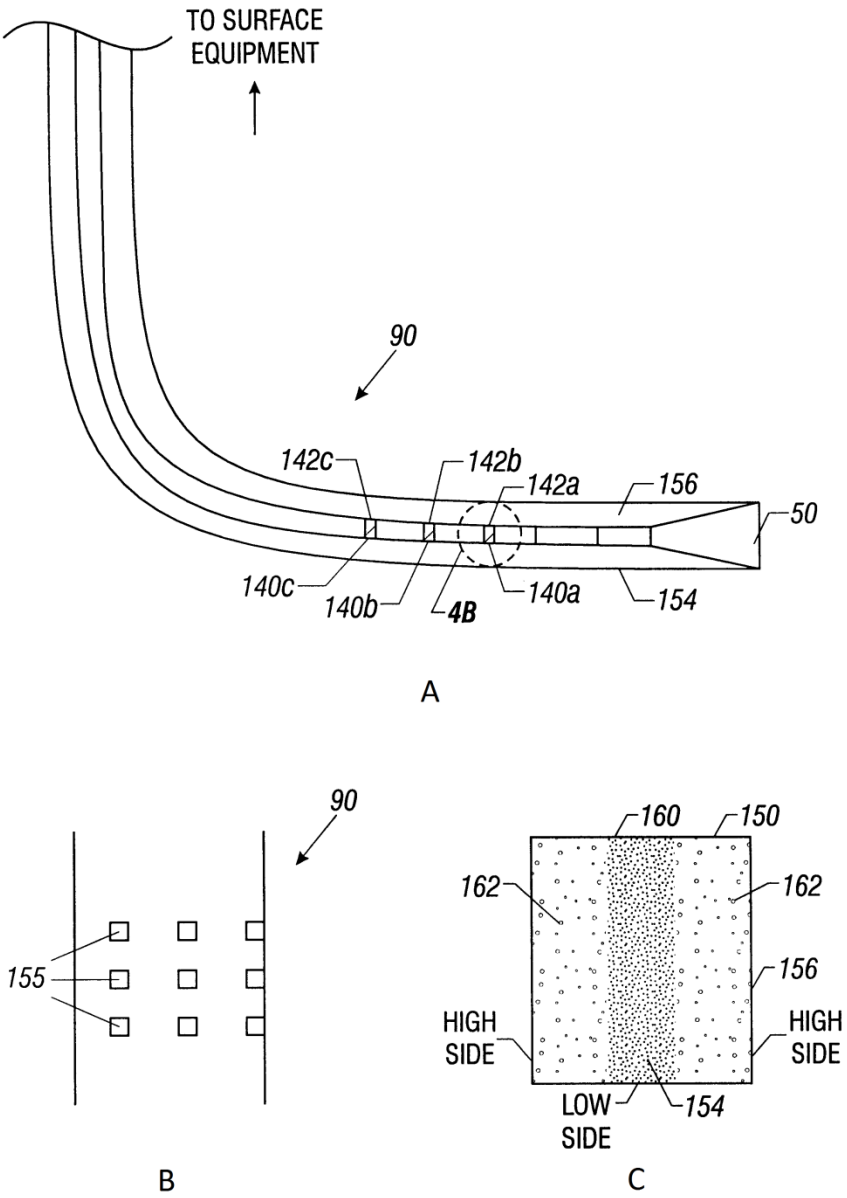

Figure 19: A: Schematic of the drill string with acoustic devices. B: Arrangement of acoustic sensor elements. C: Display of fluid characteristics obtained by an acoustic device [36]

Figure 19 A illustrates the ultrasonic sensor system which is utilized to determining hole cleaning efficiency in terms of cutting accumulation and the well borehole size. The drill string is equipped with three space out acoustic sensor arrangements (*140a-140c*) containing one or more transmitters. The ultrasonic signals are transmitted with a predetermined frequency depending on the depth of the investigation. The relative amount of solids in the drilling fluid is determined by limiting the depth of investigation to the average borehole diameter size (*142a-142c*). Each of the sensor arrangements includes a receiver to receive the transmitted signal reflected from the solids in the drilling fluid. The setup can be arranged so that each sensor element operates as transmitter and receiver. Depending on the range of axial cover that is needed, a setup such as Figure 19 B, where several sensor elements (*155*) are arranged around the drilling assembly (*90*) can be used. In order to activate the MWD sensors, the drilling operation stops temporarily. When measuring the signals from each of the sensor arrangements (*140a-140c*), the signals are further processed by the down hole processor and an image of the fluid volume (*142a-142c*) in the annulus are obtained. Figure 19 C is an illustration of a radial image captured by the sensor arrangement (*140a*). The image *150*, if rolled end to end at low side *154*, it will be the image of the volume (*142a*) around the sensor arrangement *140a*. The image shows a cluster (*160*) of ultrasonic reflections for the low side *156*, which is an indication of accumulation of solids, usually cuttings. On the high side *156* there are relatively few reflections (*162*), indicating the cuttings are flowing along the high side of the wellbore. Such measurement methods give the operator the opportunities to visualize the presence of cutting in an area of investigation. The spaced out sensors together with varying frequency, the given area of investigation, can be extended though a larger portion of the drill string and local accumulation can be found. When the driller are alarmed of such scenario, corrective actions can be started by increasing the flow rate and hole cleaning or perform a bit replacement [36].

2.3 Measurements of Drilling Fluids and Drill-Cuttings

Saasen et al. (2007) [49] described a system for automatic measurement of drilling fluids and drill-cutting properties. Automatic measurements of several drilling-fluid properties are crucial if a drilling process is to be controlled remotely. Such a system should be able to react to changes in real time and give a better control of drilling fluid parameters. A tool was designed to automatically measure several parameters and was tested on rigsite and at the Cubility Test Center in Sandnes. Drilling fluid parameters such as viscosity, fluid loss, electrical stability (ES) and pH were obtained. The particle-size distribution (PSD), volume cuttings and cutting mineralogy were also measured with the tool. Figure 20 shows the schematic setup of the drill cuttings circulation system [49].

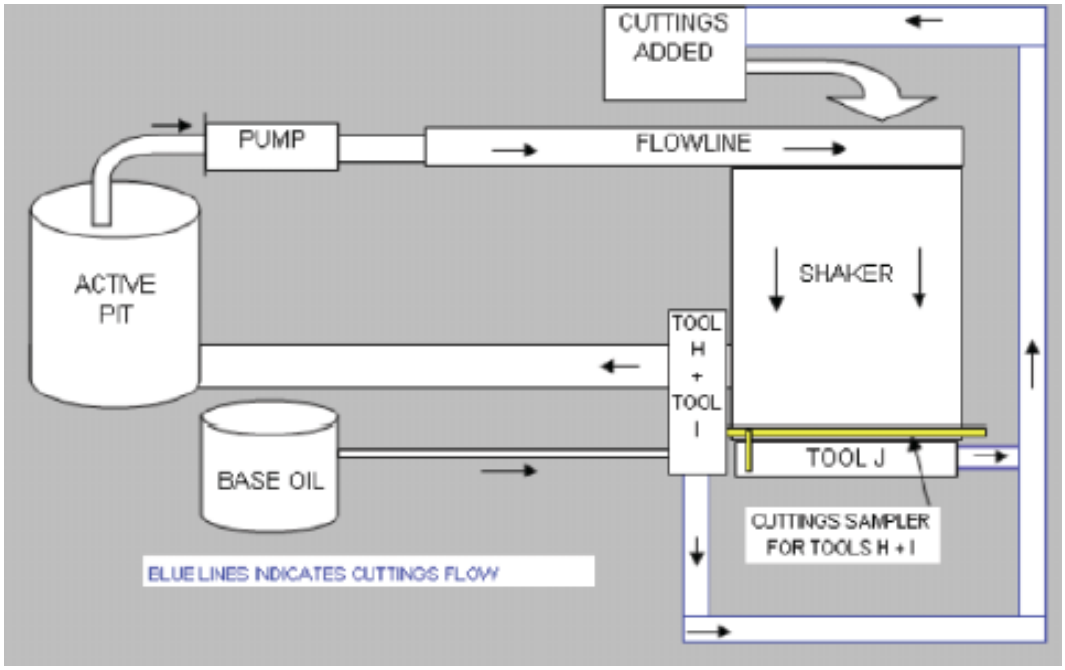

Figure 20: Illustration of a drill cuttings circulation system [49]

Figure 20 show the cuttings circulation system tested in Sandnes. The process starts from the active pit where drilling fluids are pumped at 815 L/min to the shaker unit. Sand, shale and calcium carbonate was added to the flow just before the shaker to represent cuttings or cavings from unconsolidated formations. The rocks are collected and sampled by a cuttings flow meter (Tool J). A sampler was connected before the cuttings flow meter and determines if the cuttings are actual cuttings or cavings. The cuttings sampler tool feeds the cuttings to a cuttings morphology tool (Tool H) and Roman spectroscope (Tool I) where the cuttings mineralogy is obtained. The drilling fluid properties were also measured by a similar setup to

Figure 20 and viscosity, density and PSD was found [49]. Each method of measurements will be shortly described in the next section.

Viscosity: Since drilling fluids are generally non-Newtonian with properties such as shear-thinning viscosity and viscoelasticity, simple in-line devices are not adequate. It is necessary to obtain rheograms to predict pressure losses while circulating fluids. Fluid models for Bingham and Power-law are used with parameters measured from viscosity and should ensure equivalent circulating density (ECD) control. An in-line Couette viscometer for a shear rate span of 5-1022 s^{-1} was chosen. Saasen et al. (2007) discussed the possibility of introducing ultrasound doppler effect. The conclusion was that this type of application was not ready for implementation in the field [49].

Density: The most common practice today is to measure the density continuously. A Coriolis flow meter is the preferred method in this paper. Saasen et al. (2007) states this to be the most accurate flow meter available, where density measurements are done "simultaneously" with the mass flow rate. However the Coriolis is heavily affected by gas fraction and solid content. To overcome these obstructions, a pressurized bypass loop is installed. By doing so the Coriolis can be used for pressures up to 35 bar and the accuracy increased for scenarios with solid content and gas. The use of ultrasonic methods for flow measurements was not discussed in the paper [49].

Particle-Size Distribution: The use of light diffraction is the most common method for determining PSD in the petroleum sector. A laser beam is used to expose the particles in the liquid and the shape and particle size are obtained from the scattering. This was done by applying an algorithm based on an assumed shape of each particle. Hence there is room for false values. A full-frame photo-imaging system was introduced to overcome the challenges with the laser technique. The system requires a steady flow of drilling fluids passing through the imaging section. If so, the concentration and particle morphology can be determined [49].

Another solution was suggested by Karim (2013) [52]: An ultrasound particle analyzer that is capable of on-line and in-line measurements of size distribution and solid content in drilling muds. The method is referred to as Ultrasound Extinction (USE) and utilize sonic instead of light. The system will then be able to operate with opaque fluids with concentrations as high as 70 vol%. It is operated by an electrical high frequency generator connected to a

piezoelectric ultrasonic transducer. The principle is similar to the laser diffraction, where the relative amount of material in cubic meters or kilogram are obtained. The ultrasonic waves propagating through the suspension are received by the ultrasonic receiver/detector and converted to an electric signal. The extinction of ultrasonic waves is then calculated from the ratio of signal amplitude on the generating side and the receiving side [52]. The three methods of PSD measurements are compared in Table 1.

Table 1: Summary of PSD measurement methods [52]

Method	Measurement method	Min size	Max size	Recommended for real-time	Advantages for cuttings measurements	Limitations for cuttings measurements
Laser Diffraction	Off-line At-line	0.04µm	2000 µm	No	Lab Availability	Upper size limitation
Image Analysis	On-line At-line Off-line	20µm	3000 µm	Yes	Identify particle type	
Ultrasonic Extinction	Off-line On-line In-line	0.01µm	3000 µm	Yes	Volumetric solids concentration	

In Table 1 each of the methods is compared with ways of obtaining/analyzing, minimum and maximum particle size, real-time availability and advantages and limitations for cuttings measurements.

Mud-Solids Monitor: The MSM is based on X-ray fluorescence (XRF) spectra with calibration involving two or more variables. The concentration of solid phase and liquid phases can be obtained with reasonably high accuracy. The system has been field tested and has been a subject to several articles. A typical XRF use two radioactive sources and are therefore applicable for detecting both light and heavy elements. The main concern in using this method offshore is the tight restrictions due the radioactive source, especially in terms of transportation [49].

Cuttings Flow meter: The cuttings flow meter gives the operator ability to observe the hole cleaning efficiency. The cuttings are collected in a tray at the outlet of the shakers, and basically weigh returning cuttings from the well. The tool was first used in an extended well

in Argentina in 1995 and proven reliable for hole cleaning efficiency. The total weight of the returned cuttings is converted to volume. The expected volume of cuttings is compared to the actual volume and the operator can get an indication of problems such as cavings and volume of cuttings remaining in the hole, calculated from the average rock density [49,50].

Roman Spectroscopy: A well-established method for chemical analysis and is used for identifying minerals, fluids and hydrocarbons. The obtained mineralogy can be used to identify new formations while drilling. Some formations are potentially poor formation and can induce drilling problems such as hole instability.

One important aspect of the tool is to determine if solids going through the shakers are drill cuttings or cavings from unstable formations. Saasen et al. (2007) stated that Roman spectroscopy can be used to determine formation-fluid composition [49].

The non-destructive method is an effective tool to characterize drill cuttings, with rapid analytical results in a digital format. It is suitable for automatic description of cutting components [51].

All of these instruments will result in a large quantity of real-time data and needs to be interpreted carefully by the operator. By doing this right, a smoother and more efficient method for managing fluid-and-solid control in a drilling operation can be achieved. In theory, the solution will result in a more cost efficient and safer operation, since the response-time to varying drilling environments is reduced.

3. Acoustic Methods

Acoustics is the study of sound and has a wide area of application, from designing concert halls, medicine, warfare (sonar) and industrial processes. The interdisciplinary science of acoustics concerns mechanical waves in gases, liquids and solids including vibration, sound, ultrasound and infrasound [15]. The word acoustic comes from the greek word akoustikos meaning hearing. Robert Bruce Lindsey from the Acoustical society of America earned a gold medal in 1963 for "major contributions to the knowledge of physical acoustics through research and authorship; for teaching and training acousticians; and for sustained service to the Society as an officer and Editor-in-Chief of its publications" [17]. He contributed to develop the wheel of acoustics as seen below in Figure 21, which summarizes all the various disciplines and sciences of acoustics.

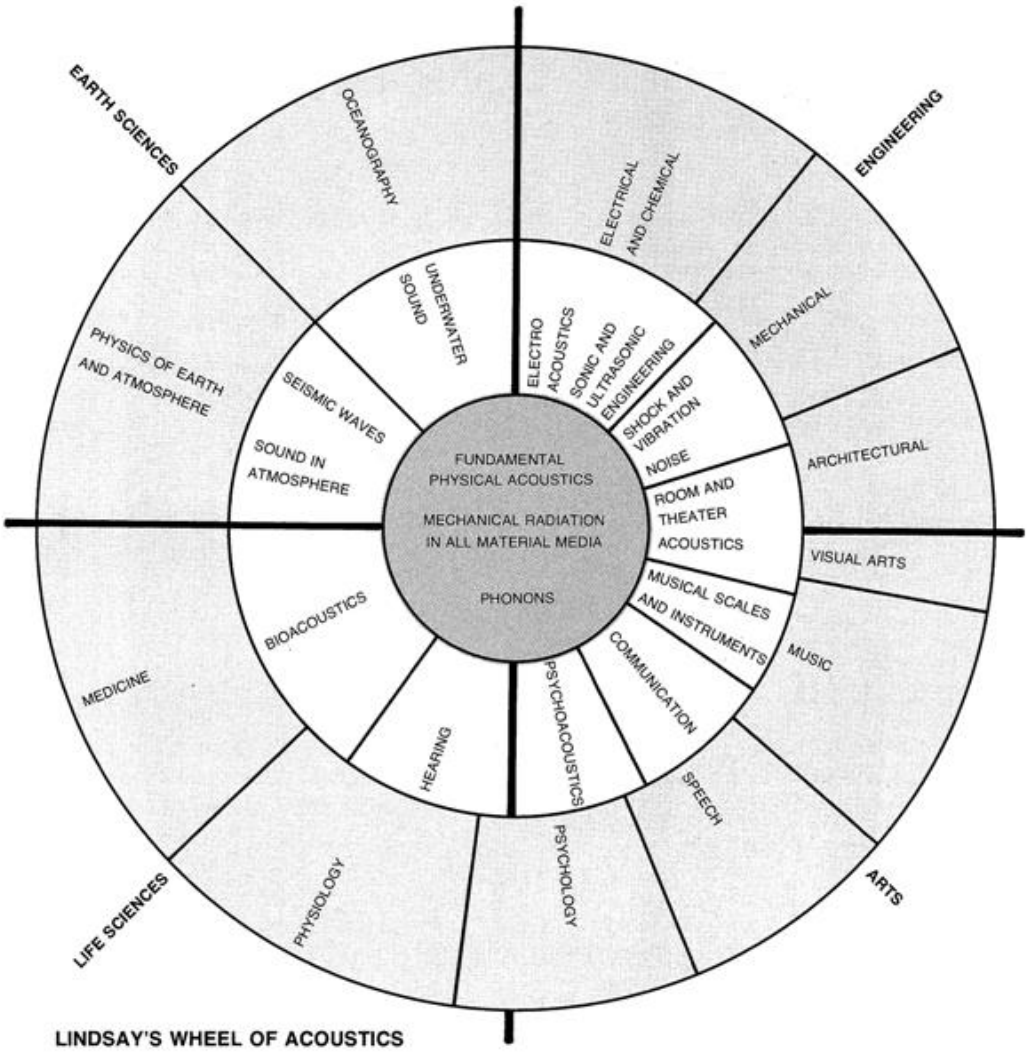

Figure 21: The wheel of Acoustics by Robert Bruce Lindsey (1964) [17]

3.1 Detection of Oversized Material by Acoustic Measurements after K. Albion (2009) [18]

Acoustic measurements are especially useful in process monitoring of sand and oversized material in oil production pipelines. By placing acoustic sensors strategically and applying signal analysis techniques, in-line detection is possible. The sensors are mounted outside the pipe and do not interact directly with the flow. The non-intrusive method is necessary where oil producing flows are subjects to high temperature and pressures. The harsh environments will easily cause damage to sensors mounted inside the pipe.

A well-known method is using Acoustic Emissions (AE) from rocks colliding with pipe wall. The noise is recorded with microphones and processed. Albion et al. (2009) [18] is one of several studies on material detection in a hydrotransport system. By using prepolarized electric condenser microphones, the sound pressure fluctuations were transformed to capacitance variations and further to electric voltage signals. The oscillating voltage is proportional to the original pressure fluctuations. For signal analysis Albion et al. (2009) used Kurtosis, a measure of relative peakedness (width of peak) of a distribution. The use of Kurtosis was used to distinguish collisions from noise and is given by

$$KRT = \frac{\sum_1^M (y - \bar{y}^4}{M\sigma^4} - 3 \tag{24}$$

where y is the signal value, ȳ is the signal mean, σ is the signal standard deviation and M is the number of points in the signal. A threshold limit of KRT=10 was used to distinguish slurry noise from collisions in the experiment. If the Kurtosis value exceeds 10, a collision has occurred.

The microphones need to be mounted so the rocks collide at approximately same location for every run. This was achieved by placing them after a bend in the pipe. The experimental setup consisted of a 50 mm ID stainless steel pipe with a wall thickness of 4 mm. The schematic is illustrated in Figure 22.

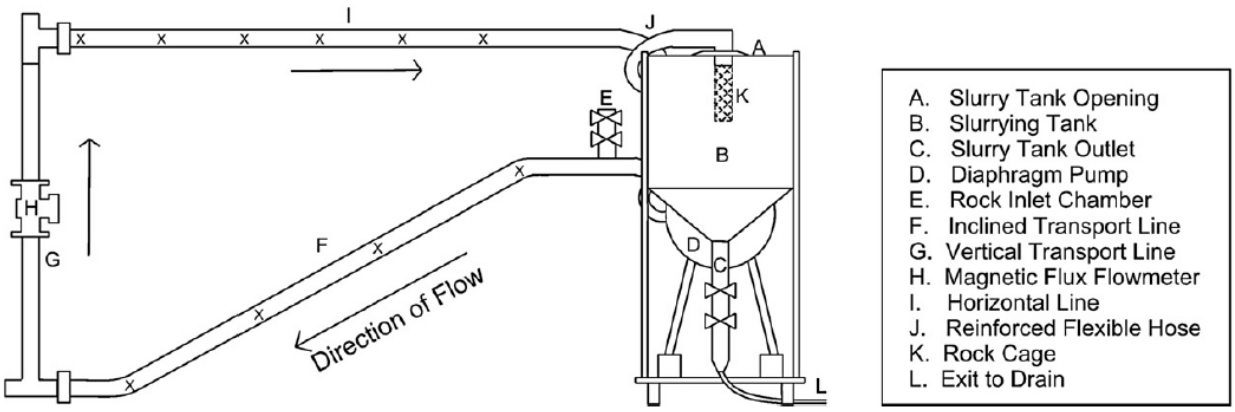

Figure 22: Experimental setup by Albion et al. (2009), where X indicates the microphone setup [18]

Water and solid is pumped though the loop by a diaphragm pump. To monitor the flow velocity, a magnetic flux meter (G) was mounted. The inclined section (30º) was 2.75 m, the vertical pipe was 1.7 m and the upper horizontal section was 3.6 m. In order to add rocks and retrieve them, a rock inlet chamber and rock cage was used. Vibrations from the pump needed to be reduced, so a reinforced flexible hose was mounted [18].

The slurry consisted of various concentrations of silica sand with Sauter-average diameter of 180 µm, density of 2650 kg/m^3 and terminal velocity of 0.022 m/s. The concentration of the slurry was tested from 10 to 50 wt%, with an interval of 10 wt%. Flow velocities of 1, 2, 3 and 3.5 m/s was used. The effective viscosity of the slurry needed to be measured every 10th interval and ranged from $1.13 \cdot 10^{-3}$ to $2.90 \cdot 10^{-3}$ pa·s. 13 types of rocks, with varying shape and density, as seen in Figure 23, was added to the loop [18].

Rock	Shape	Volume-equivalent diameter (mm)	Albertson shape factor (–)	Clift shape factor (–)	Density (kg/m^3)	Experimental terminal velocity (in water) (m/s)
A	Round	19.2	0.718	0.312	2735	0.75
B	Round	16.8	0.709	0.342	3160	0.75
C	Round	17.9	0.567	0.274	2867	0.63
D	Round	15.1	0.423	0.222	3111	0.63
E	Round	12.0	0.568	0.237	3111	0.75
F	Round	11.5	0.694	0.474	3250	0.63
G	Round	10.5	0.676	0.384	2750	0.94
H	Round	9.1	0.623	0.243	3125	0.75
I	Angular	18.3	0.724	0.318	2700	0.46
J	Angular	17.5	0.675	0.302	2482	0.63
K	Angular	15.4	0.608	0.252	2726	0.75
L	Angular	14.2	0.486	0.249	2133	0.75
M	Angular	9.1	0.591	0.166	3700	0.54

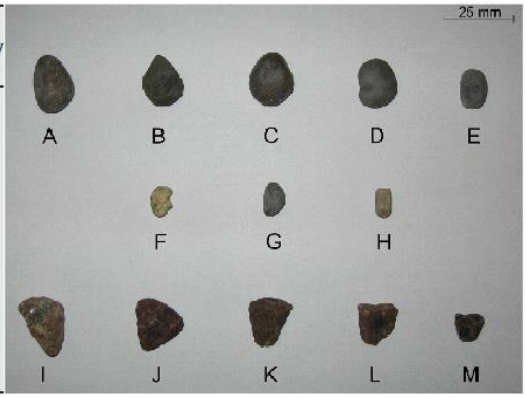

Figure 23: Thirteen different rocks and their properties [18]

For each concentration of slurry, 45 liters of water was added to the storage tank to prevent the sand to settle. As the flow was steady, the acoustic measurements started. The recorded

frequency was set to 40,000 Hz for each sensor and preamplifiers were used to record the acoustic signals. The distance from the vertical bend to the horizontal microphones were set to 0.03, 0.50, 1.00, 1.50, 2.00 and 2.50 m and the raw signal were recorded by National Instruments LabView software before Kurtosis was applied. The amplitude of the peaks in raw data corresponds to the magnitude of the peaks of Kurtosis. The time interval was set to 0.010 s [18].

The recorded data for slurry velocity of 3 m/s and 30 wt% illustrated in Figure 24 and each of the microphones show a significant peak between 5.5 and 6.5 s. This is the noise from rock C, described in Figure 23, colliding with the pipe wall at the horizontal bend [18].

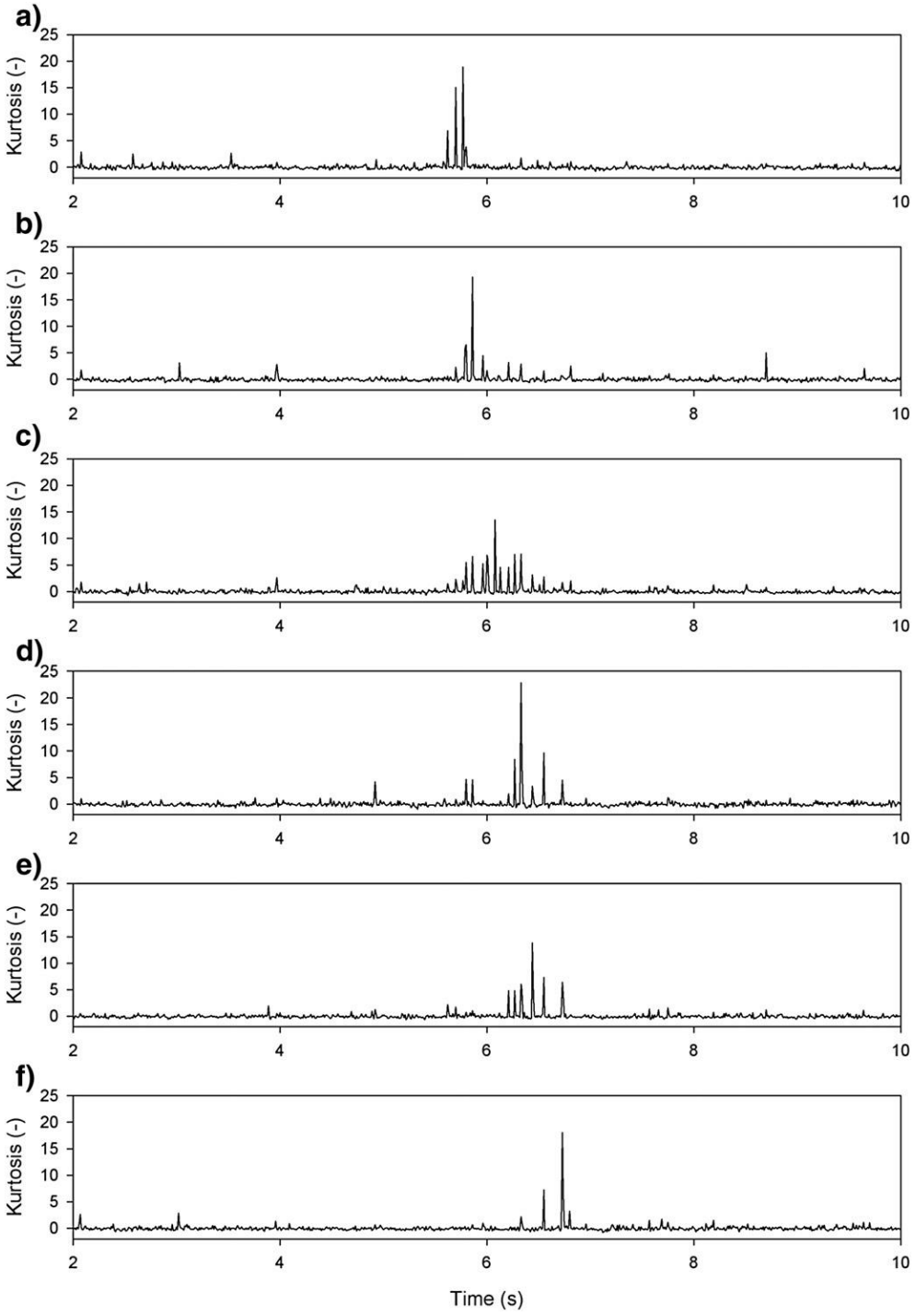

Figure 24: Kurtosis of Rock C [18]

The microphones located closest to the point of collision shows higher peaks of Kurtosis. Larger rocks would also have an impact on the peaks, as the force of impact is greater. An important observation is that a small rock colliding near a microphone showed a higher peak than a large rock colliding far away. Hence several microphones should be used as the peak size decrease with distance. The propagation of the rock increased as the slurry flow velocity increased and for the lowest velocities (1 m/s) the rocks would not be able to travel the

inclined pipe unless the concentration is 40 wt% or higher. The number of collisions is also affected by the slurry velocity, where lower slurry velocity increases the rock-wall collisions. By increasing the rock sizes, the collisions occurs more often as they occupy more space in the pipe and are more difficult to keep suspended. Albion et al. (2009) also discussed the effect of angular shape rock versus rounded rocks; the angularity cause more turbulence in the fluid and more frequent collisions. The first microphone in start of the horizontal section (0.03 m) is the most important sensor and recorded 77.2% of the rocks, throughout the experiment. By increasing the number of microphones up to ten, the accuracy increases for each microphone added. 100% accuracy was achieved at ten microphones. By classifying oversized rocks as:

$$\frac{Rock\ Diameter}{Pipe\ Diameter} > 0.25 \tag{25}$$

these can be detected by three or four of microphones in the loop. Albion et al. (2009) created a model for the critical measurement location of microphones for the various slurry velocities:

2 m/s: 0.03, 0.50 and 1.00 m in the horizontal line
3 m/s: 0.03, 0.50 and 1.00 m in the horizontal line
3.5 m/s: 0.03, 0.50, 1.00 and 2.00 m in the horizontal line [18].

The pump used in this experimental setup caused some noise, but by using Kurtosis this noise can be removed even if the peaks from the rock collision are similar to the pump noise [18].

4. Ultrasonic Methods

Ultrasonic measurements are well established techniques in several industries for purposes such as material testing (non-destructive testing), medical testing (ultrasound), flaw detection and oceanography [1]. Ultrasound is basically vibrations of frequencies greater than 20,000 Hz, which exceeds the upper limit of the human ear. The applications of ultrasonic methods are environmentally friendly, non- invasive and useful for characterizing liquid-particle flows for real-time measurements. Some multiphase flow parameters measured by ultrasonic are concentration of solids, flow speed and instabilities in turbulent flow regimes [19]. Through the years, several studies and models have been done. In this chapter some important equipment and physical properties are reviewed followed by a literature study of relevant ultrasonic methods.

4.1 Physical Properties and Equipment

4.1.1 Transducers

Ultrasonic transducers are devices used for converting energy into ultrasonic vibration. In order to produce these sound waves, mechanical movement or oscillations of a crystal (quartz, ceramic or Rochelle salt) by electrical pulses. This effect is known as the piezoelectric effect and was first discovered by the Pierre and Jacques Curie in 1880. Shortly after, in 1881, they proposed the reverse effect by converting the energy back to its original form. Transducers are often classified by the energy source the waves are being transmitted by. Mechanical devices, such as whistles and ultrasonic cleaners, are limited to lower ultrasonic frequencies. The most common used transducers are electromechanical such as piezoelectric and magnetostrictive. The Piezoelectric transducer is far more versatile since it operates over the entire frequency range at low voltages and different shapes can be applied for specific applications, such as focusing at specific points. The magnetostrictive transducer is restricted to lower frequency ranges and is applicable for ultrasonic cleaning and ultrasonic machining operations. Both the piezoelectric and the magnetostrictive can be used as receivers for ultrasonic vibrations and for applications for more than one transducer [20].

The Pulse-echo principle is a very common technique for ultrasonic measurements. The conversion of electricity into sound refers to the *pulse* and conversion of sound into

electricity refers to *echo*. The pulse-echo method is based on transmitting ultrasonic waves and receiving echoes with a single transducer. Since only one transducer is needed for this method it requires only access from one side and is cost effective. The returning pulses may be received as a single reflection or multiple reflections. The sound velocity and attenuation can both be measured as the amplitude varies and the travel time is recorded.

By using a transmitter and a receiver on each side of a pipe, the through-transmission method can be used as the sound goes through the medium and any interruptions along the path are recorded on the other side.

The Pitch-catche mode is based on two transducers where the waves are transmitted in any angle and received by the second transmitter as reflected energy.

4.1.2 Frequency

The frequency (f) refers to the number of complete cycles per unit of time (s); one cycle per second is equal to one Hertz. The time to complete a cycle is the Period (T) and is measured in seconds. The relationship between frequency and period is given

$$f = \frac{1}{T} \tag{26}$$

The bandwidth refers to the range of frequencies the transducer can operate under. A transducer with broad frequency range will have a higher resolving power, but less penetration compared to a transducer with smaller frequency range. The transducers are typically divided in low frequency transducer (0.5–2.25 MHz) and high frequency transducers (2.25–25.0 MHz). The choice of frequency is crucial for getting the best resolution [21]. In literature, the term Pulse Repetition Frequency (PRF) is often used to avoid any confusion and is the number of pulses per unit time (s). This unit is often used in radar technology.

4.1.3 Wavelength

Ultrasonic vibrations travel in forms of a wave is much similar to light but they cannot travel in vacuum. The waves need an elastic medium such as liquids and solids in order to

propagate. When comparing sound waves to ultrasonic waves, the wavelength (λ) is much shorter and can reflect of much smaller objects. Figure 25 below shows the relationship between the period and wavelength.

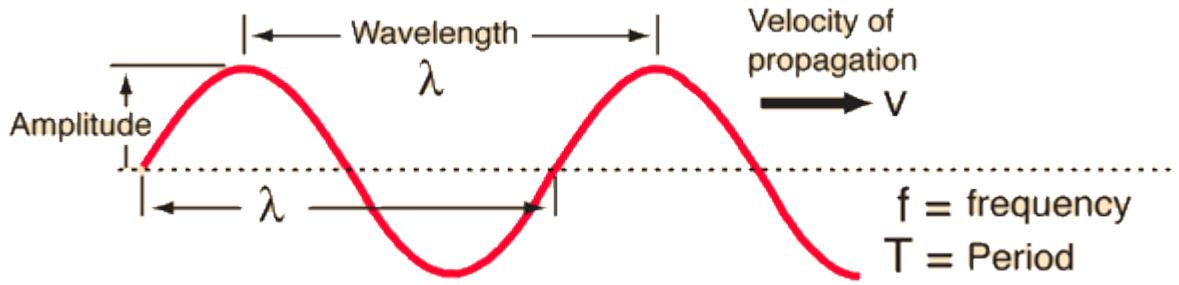

Figure 25: Relationship between amplitude, velocity, wavelength and period

As the wave propagates though the medium in the form of a sine wave, the relationships can be determined as the x-axis as a function of time or distance. For determining the wavelength of the graph, it must be a function of distance and is therefore given by

$$\lambda = \frac{v}{f} \tag{27}$$

From equation 27: Change in frequency will result in change of wavelength. This change in wavelength is important specially in ultrasonic testing, such as Non-destructive testing. The amplitude describes the maximum variation from the equilibrium position or value.

4.2 Literature Study of Ultrasonic Measurements

4.2.1 Attenuation measurements

Attenuation in colloids is described by the loss of energy as sound travels through a medium. The loss of intensity has an impact on the amplitude as the wave propagates and is an important parameter in ultrasonic measurements. Attenuation comprises of absorption and scattering and is highly dependent on the frequency domain. Absorption is the conversion of acoustic energy to thermal energy and are the main cause of attenuation. The scattering is caused by change in direction of acoustic energy from the incident beam.

Wrobel (2012): for a given particle size the absorption is dominant for low frequencies, while scattering in ultrasound is dominant for high frequencies. There is also an overlap in moderate frequencies from dominating absorption to scattering. The critical frequency gives the frequency of maximum attenuation and is related to particle size or inter-particle distance [19].

The determination of attenuation in liquids containing particles is a subject of many studies. Stolojanu and Prakash (2001) [24] wrote an article published in the Chemical Engineering Journal: *Characterization of slurry system by ultrasonic techniques*. By using ultrasonic sensors, the particle concentration and variation in size distribution of a liquid-particle solution was determined. The variations in velocity and attenuation can be measured by the Phenomenological model approach by Ulrich (1947) [22]. The model is applicable with small particle sizes and near the wavelength of the acoustic signal or the wavenumber $kr << 1$. The acoustic velocity was then determined with the average values of compressibility and density. By including the effect of fluid viscosity and particle size, Ament (1953) [23] improved the equation. By doing so, an effective density equation concluded that an increase in particle size in a liquid-solid flow would result in increased ultrasonic velocity for a given solid concentration and frequency. The energy loss or transmission loss are as mentioned earlier in this chapter due to absorption and scattering, but also due to reflection, refraction and diffraction. For particles smaller than the pulse wavelength, the scattering phenomena are the dominant reason for energy loss. For larger particles, reflection and refraction at the solid-liquid interface were considered. The study was based on investigating variations in velocity, attenuation and average frequency for loadings up to 45 vol%. The particles used in the experiment were glass beads with the sizes 35, 70 and 180 μm. The experimental setup

included a 0.5 m high plexiglass with diameter of 0.1016 m. A mechanical stirrer was used to maintain a homogeneous suspension and the revolutions per minute (rpm) needed was obtained from Zwietering (1957) [25]. He investigated the required stirring speed to keep a suspended condition. The rpm was set between 800 and 2000 rpm and usually 10% above the value derived from Zwietering (1957). Two ultrasonic devices were used as a transmitter and receiver at 0.5 m from the bottom and 0.02 m off the center. The transducer was ceramic based and a 3 MHz center frequency of 50% bandwidth. The pitch-catch mode was used and high energy pulse (800 µJ) was needed for the dense suspension. A digital Personal computer and Oscilloscope was also used in order to control the system parameters (pulse voltage and energy) and visualizing/analyzing of the received signal [24].

The variation of acoustic speed in increasing concentrations of three different particle sizes, was the first study. The result is seen in Figure 26.

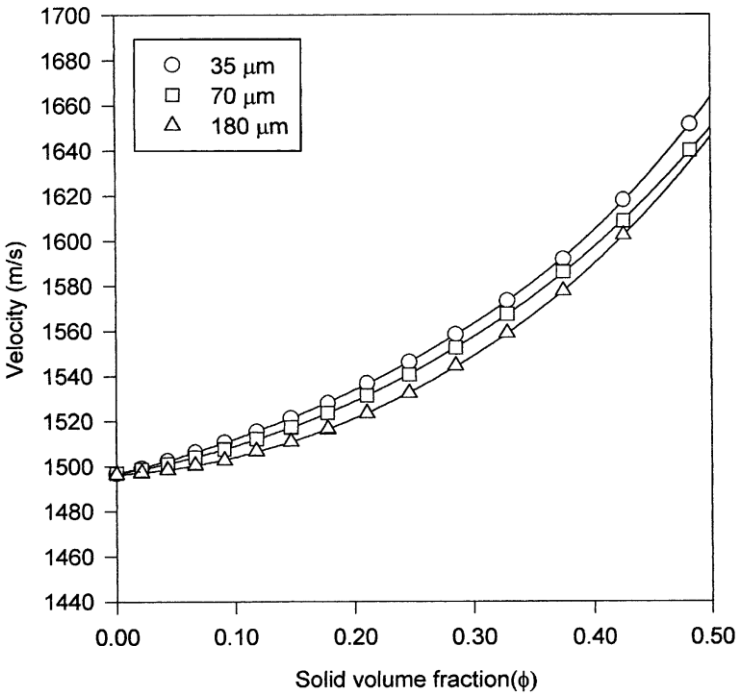

Figure 26: Variation in acoustic velocity with increasing solid concentration for the three different particle sizes [24]

As the concentration increased to 0.05 vol% there was only small changes in the acoustic velocity. When the concentration increased further the velocity increased in a higher rate. From Figure 26 the velocity in the larger particle size (70 and 180 µm) systems are less than the small particle size system concentrations. For the suspensions with fine particles and small wavenumber ($kr<<1$), the system can be thought of as homogeneous and the phenomenological model can express the sound speed by

$$v = \frac{1}{\sqrt{\rho_{eff}\beta_{eff}}} \tag{28}$$

where ρ_{eff} is the effective density and β_{eff} is the effective compressibility of the mixture. These are based on the linear averaging using the volume fraction of dispersed particles, φ [26]:

$$\rho_{eff} = \varphi\rho_2 + (1-\varphi)\rho_1 \tag{29}$$

$$\beta_{eff} = \varphi\beta_2 + (1-\varphi)\beta_1 \tag{30}$$

where subscript 1 refers to the liquid phase and subscript 2 refer to the dispersed phase. In the literature there are several cases where ρ_{eff} and β_{eff} relies on other parameters such as fluid viscosity and particle size, not only the volume fraction and dispersed particles.

Stolojanu and Prakash (2001) [24] compared their experimental results with the earlier studies from Urick (1947) [22], Ament (1953) [23], Harker together with Temple (1988) [26] and Atkinson and Kytomaa (1992) [27]. The results are illustrated in Figure 27 below.

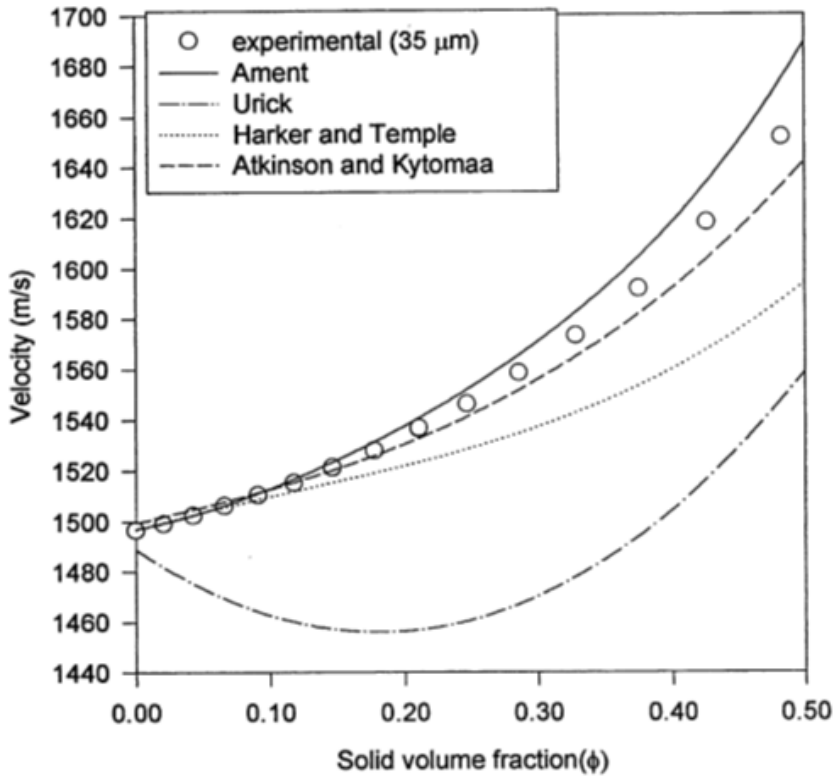

Figure 27: Experimental results from Stolojanu and Prakash (2011) compared with Ament (1953), Urick (1947), Harker and Temple (1988) and Atkinson and Kytomaa (1992) [24]

Figure 27 shows good alignment with most of the earlier studies up to 12-13 vol%. As the volume fraction increases further, the studies of Harker and Temple shows some deviation from Urick (1947), Ament (1953) and the experiments of Stolojanu and Prakash (2001). The predicted low increase in acoustic velocity by Harker and Temple (1988) is due to lack of effect by particle diameter. The result is decreasing acoustic velocity as the particle size increases [24]. The change in acoustic velocity with increasing particle concentration can be correlated by using Urick's equation

$$\frac{1}{V^2} = \frac{1}{V_0^2} + \beta_1\varphi + \beta_2\varphi \tag{31}$$

where β1 and β2 are determined by experiments and are functions of particle size. By creating calibration lines between the known particle sizes, these calibration curves can be used to determine slurry concentration from acoustic velocity in suspensions [24].

For the measurement of attenuation in order to characterize the mixture, the attenuation coefficient was used and described by

$$\alpha = \sum_{i=1}^{n} \alpha_1 = -\sum_{i=1}^{n} \frac{1}{L} \ln\left(\frac{A_i}{A_{oi}}\right) \tag{32}$$

where A_{oi} is the amplitude level before adding the solids, and A_i is after solids are added. The experiments consisted of adding particles of 70 and 180 µm to a 15 vol% suspended system with 35 µm particles. The result was plotted by Stolojanu and Prakash (2001) and is shown in Figure 28.

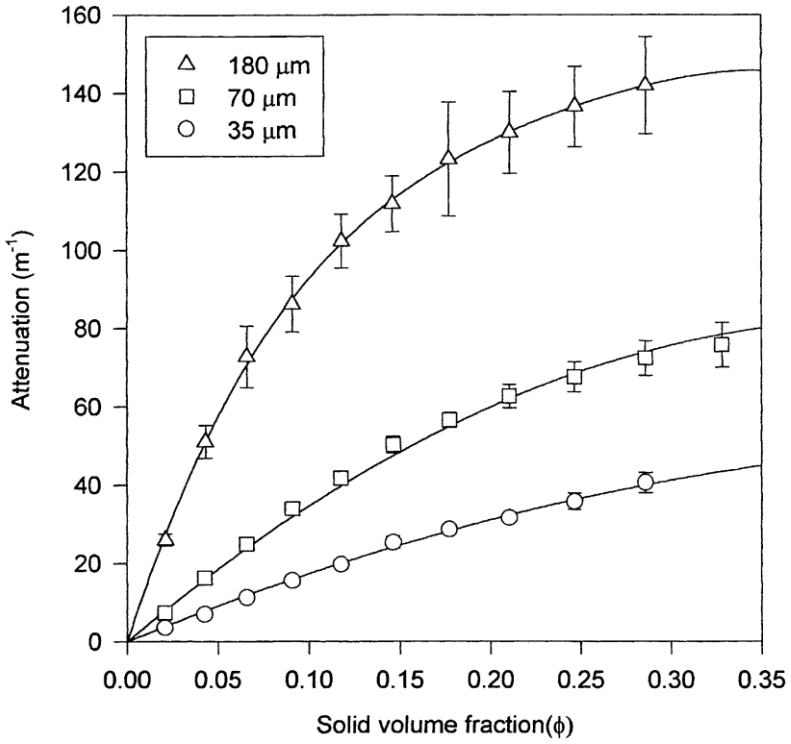

Figure 28: Attenuation as a function of slurry concentration [24]

The increase in solid fraction causes increasing of the attenuation coefficient is presented in Figure 28. The increase in attenuation of the three cases is quite different. The system where particles of 180 µm are added will have a larger impact on the attenuation, than the 70 and 35 µm respectively. The rate of increase in attenuation is quite high for the 180 µm until 0.15 vol%. Beyond this point the increase in solid concentration becomes less significant for the attenuation. The scattering phenomena caused a deviation in the linear attenuation as shown in Figure 28. The dominant scattering occurred as the kr increased at the same frequency due to the increased particle size.

Epstein and Carhart (1941) [28] developed an estimation of attenuation in liquid-solid suspensions and was later confirmed by Stakutis et al. (1955) [29] by applying the study to other types of solid and not only elastic solids. They both considered the attenuation coefficient to consist of three components

$$\alpha_p = \alpha_{sc} + \Delta\alpha_V + \alpha_{vis} \tag{33}$$

where α_{sc} is a scattering component, $\Delta\alpha_V$ is the correction for large kr in terms of absorption and α_V is the absorption due to viscous drag. In the studies where particle density is much higher than the suspended medium, the thermal absorption, α_{th}, is very small compared to the viscous drag and can be discarded [24].

The attenuation coefficient was calculated and compared with the experiments of 35, 70 and 180 μm particles in the increasing solid volume fraction. The equation used by Stolojanu and Prakash (2001) is given by

$$\alpha_p = \varphi k(\delta - 1)Re\left[\frac{i + b - ib^2/3}{\delta - i\delta b - (2+\delta)b^2/9}\right] + \frac{1}{3}\phi k^3 {d_p}^2 Re\left[\frac{10}{9b} + \frac{23^i}{4b^2}\right] + \frac{1}{3}\phi k^4 {d_p}^3 \cdot \left[\left(\frac{\delta - 1}{\delta - 2}\right)^2 + \frac{1}{3}\left(1 - \frac{3B}{3\gamma_L - 2\mu_L}\right)^2\right] \tag{34}$$

where ϕ is the solid volume fraction, k is the ultrasound wavenumber (m^{-1}), $\delta = \rho_f/\rho_s$, $b = [(i\omega\rho_f/\eta)^{0.25}d_p]$, d_p is the particle diameter (m), B is the bulk elastic modulus (Pa) and μ_L and γ_L are Lame elastic constants of the particles. Figure 29 shows the comparison of the calculated attenuation and the results from the experiments of different particle sizes.

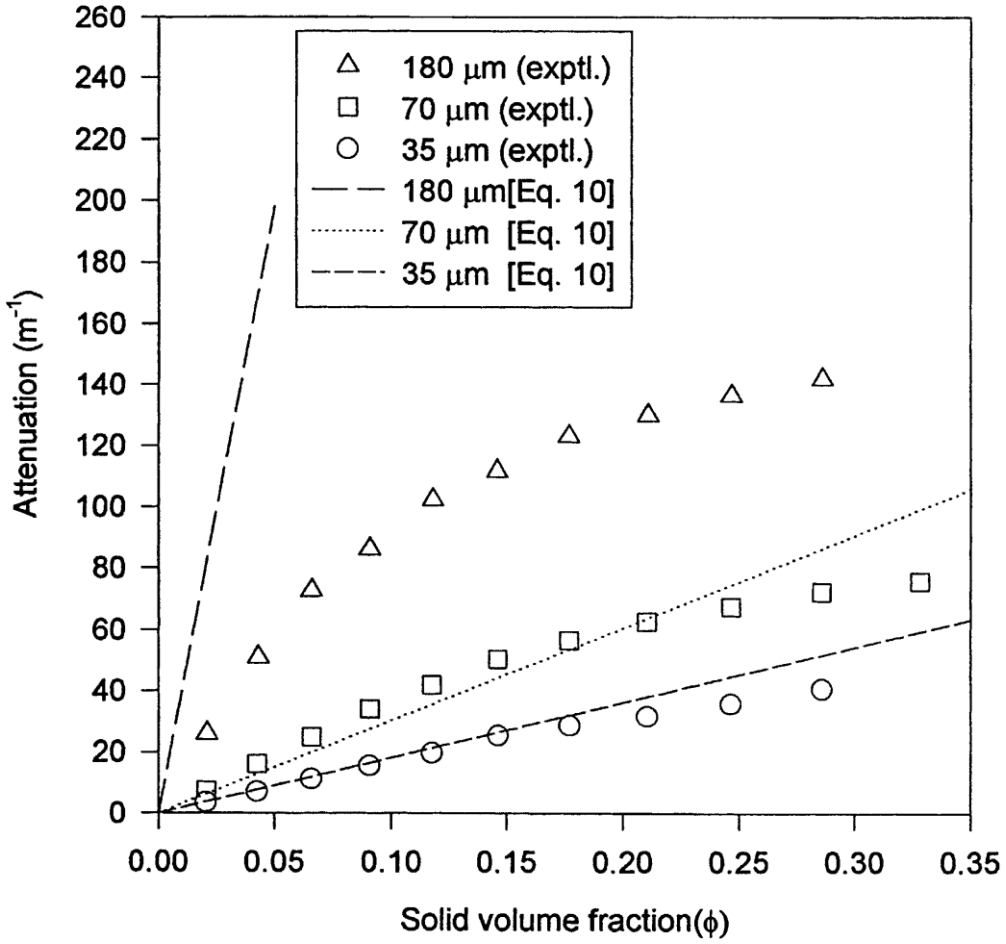

Figure 29: Experimental attenuation vs theoretical attenuation for varying particle sizes [24]

In Figure 29, the equation 34 showed a good correlation with the experiments for 35 and 70 μm particles up to 0.25 volume fraction. When the volume fraction increased further, the equation appeared less successful. For the larger particles of 180 μm the correlation were rather poor and showed false results throughout the volume fraction. Stolojanu and Prakash (2001) stated that the poor results could be due to the high wavenumbers (>1) for this particle size.

After the early work of Epstein, Carhart, Allagra and Hawley also known as the ECAH, there is still no single theory that gives a satisfactory acoustic theory for particulates. Dukhin and Goetz (2002) [30] stated that the ECAH fails since the theory is not applicable for concentrated solutions by excluding particle-particle interactions. Dukhin and Goetz (2002) developed the superposition theory and stated there should be six different mechanisms of sound attenuation with colloids; viscous, thermal, scattering, intrinsic, structural and electrokinetic. The total sound attenuation α_T can then be determined

$$\alpha_T = \alpha_{vis} + \alpha_{th} + \alpha_{st} + \alpha_{sc} + \alpha_{int} \quad (35)$$

Viscous mechanism is related to the shear waves generated by the particle oscillating in the acoustic pressure field. The difference in density of the particle and the medium is the reason for the shear waves and the density contrast causing particle motion. The shear friction cause a loss of acoustic energy and is a dominating effect for rigid particles less than 3 µm diameter [30].

Thermal mechanism is related to the temperature gradients which are generated near the particle surface. The gradients are results of thermodynamic coupling between temperature and pressure. Thermal losses are dominant for ka up to 0.5, where k is the wavenumber and a is the particle diameter [30].

Structural mechanism arises when particles are connected in a network. When they are joined together the oscillation of the inter-particle bonds causes additional energy dissipation and links acoustics to rheology [30].

Scattering mechanism occur due to reflection of acoustic energy caused by particles. The amount of sound will not reach the receiving transducer due to this reflection and effects the overall attenuation. The scattering phenomena are most significant for systems containing particles exceeding 3 µm and ka larger than 1 [30].

Intrinsic mechanism is the loss of energy due to interaction of a sound wave with material of the particles and the medium. It is considered as homogeneous phases on a molecular level. When the overall attenuation is low, the intrinsic phenomena must be considered, especially if the particle size is small and volume fractions are low [30].

Electrokinetic mechanism is connected to the oscillation of charged particles in the medium. This leads to generation of an alternating electrical field and is basis for electro-acoustic measurements. This phenomena can however be neglected in acoustic measurements, due to low contribution on the total attenuation [30].

4.2.2 Velocity measurements

Velocity measurements of flow by using flow meters can be done by using transit time differentials and Doppler shift method. These flow meters are reviewed in *chapter 5.1.1*. Ultrasonic Velocity Profile (UVP) and Particle Image Velocimeter (PIV) are used to measure the velocity of particles in a suspension rather than the fluid velocity. In the next section these two methods are described both as individual methods and simultaneously.

Ultrasonic Velocity Profile (UVP) is based on the Doppler Effect and detection and processing of echoes from ultrasound pulses that are reflected by the particles in the fluid. The Doppler Effect or Doppler Shift is defined as the change in frequency of a wave relative to the point of observation and the source. The ultrasonic pulse is emitted from an transducer along a measuring line and the same transducer measure the frequency of the reflected waves. The waves are typically short waves and all velocity profile information is contained in the echo. The measurement of travel time gives information on position of the scatted volume.

The Doppler shift is given by

$$U = \frac{c f_d}{2 f_o} \tag{36}$$

where U is the velocity in the measured line of the ultrasonic beam [m/s], c is the speed of sound in the medium [m/s], f_d is the Doppler shift [Hz] and f_o is the transmitting frequency [Hz]. The information on position is obtained from the delay in time from the starting pulse burst to the receiving point and is given by

$$X = \frac{c\tau}{2} \tag{37}$$

X is the position from transducer to the scattered particle. τ is the time between the signal is transmitted and received at the transducer.

The practice of the measurement consists of processing the echo signal at 128 times instants in parallel. The dataset is then converted to velocity profile $V(x_i)$.

Takeda (1995) described the principle of ultrasonic velocity profiling in an article published for *Experimental Thermal and Fluid Science* [32] and is seen in Figure 30.

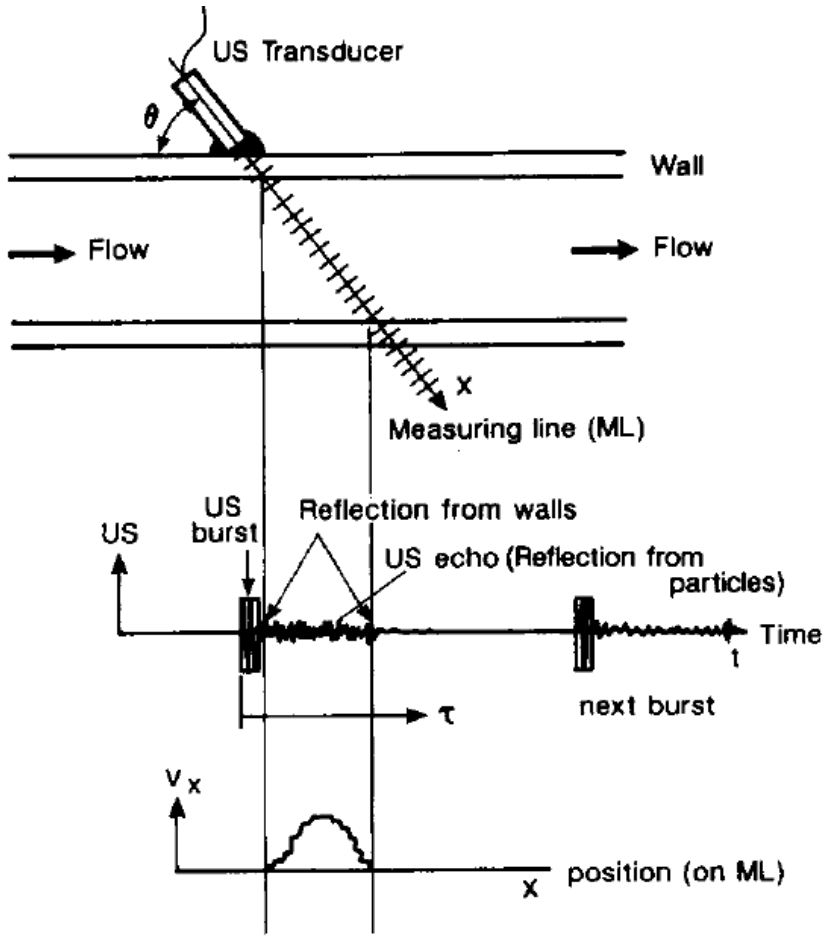

Figure 30: Principle of UVP [32]

Figure 30 shows how the transducer is set in an angle to the pipe and ultrasonic beam is propagating, noted as Measured Line (ML). The middle sketch illustrates the echo signal and the bottom sketch is the reconstructed velocity profile [32].

Rabenjafimanantsoa et al. (2005) [33] used Ultrasonic Velocity Profile (UVP) monitoring to study turbulence structures over particle beds and a setup similar to Figure 30 was used. The transducer was set with 12 degrees angle to the vertical. The loop used in the experiments consisted of a horizontal section and 5 degrees inclined section. Pipe inner diameter of 40 mm and sections of 1,5 meter pipes were connected. In order for the liquid to circulate a mainean screw pump were used. Other main elements used in the loop were: a hydroclone for adding particles, a Coriolis flow meter to measure the flow rate, a pressure column to reduce the pressure variations from the pump, a venture mixer to ensure heterogeneous slurry. In addition to a transducer, a multiplexer box, a PC and a digital oscilloscope were parts of the

setup before starting the experiments. A total of 1000 series with 128 channels were recorded above the dune structures of spherical glass beads. The results from the UVP experiment with water are seen in Figure 31. Color coding from blue to red indicates the flow velocity, where blue indicates reversal flow, green color represent zero velocity and the red color represent positive velocity.

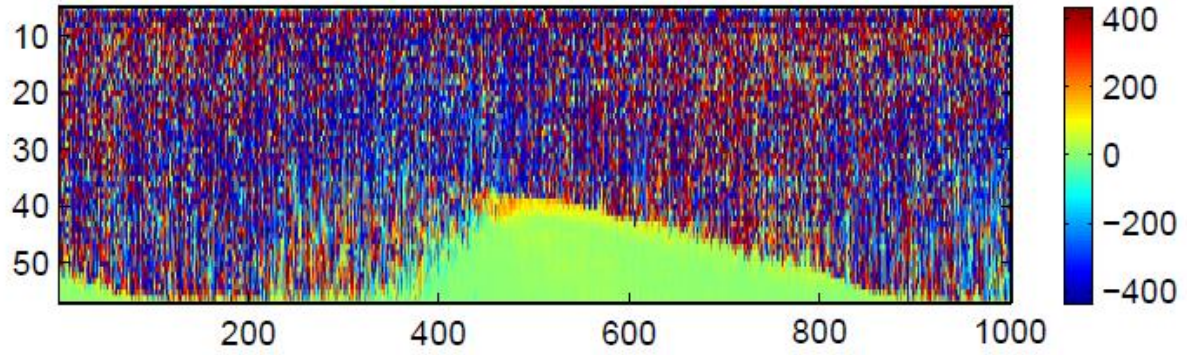

Figure 31: Velocity profile over a dune structure. Medium is water with velocity of 0.27 m/s [33]

In Figure 31 the green coding clearly shows the dune structure with zero velocity, and some reversed flow are observed, but not clearly. The vertical axis is channel depth [cm] and horizontal axis is number of profiles. The flow of water going right to left had a velocity of 0.27 m/s. Rabenjafimanantsoa et al. (2005) increased the velocity of the flowing water to almost the double. The reversed flow was now appearing clearer and the dune structure decreased in height.

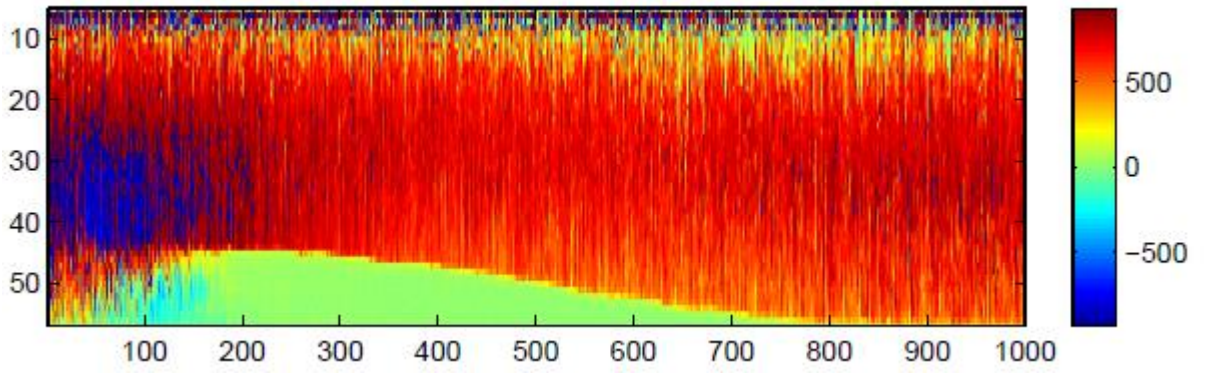

Figure 32: Velocity profile over a dune structure. Medium is Polyanionic cellulose (PAC) with velocity of 0.46 m/s [33]

The reversed flow seen in Figure 32, is dominant in the profile 10 to 200, in the horizontal axis. This is right above the dune crest where the particles are partly following the reversed flow [33].

The application of UVP were successfully applied and gave information on particle bed dynamics, liquid-particle flow profile and turbulence intensity.

Particle Image Velocimeter (PIV) is also a method used for velocity measurements, or more specific particle velocity vector in a given area. It is based on the principle of inserting artificial particles to the flow and trace the displacement of the markers or tracers. The artificial particles are small enough to not affect the flow and should have a neutral buoyant weight. Instantaneous images can be obtained by a pulse light source together with an image recording system. A powerful light source is used to illuminate the plane twice in a short time interval. The images are recorded by a camera and divided into sub windows also referred to as interrogation areas. The cross correlating the two interrogation areas of particles during the short time interval give the displacement of the tracers as 2-D velocity. In order to determine the particle velocity in PIV studies, complex software is needed. Each of the frames recorded by the camera represents a freeze of the flow in time [34].

Figure 33 shows dampened vortex structures in a jet flow situated in the profile between 100 and 200 in the horizontal axis. Further, the velocity vector can be plotted in a velocity contour and the differences in velocities are much clearer and can be seen in Figure 34 [3].

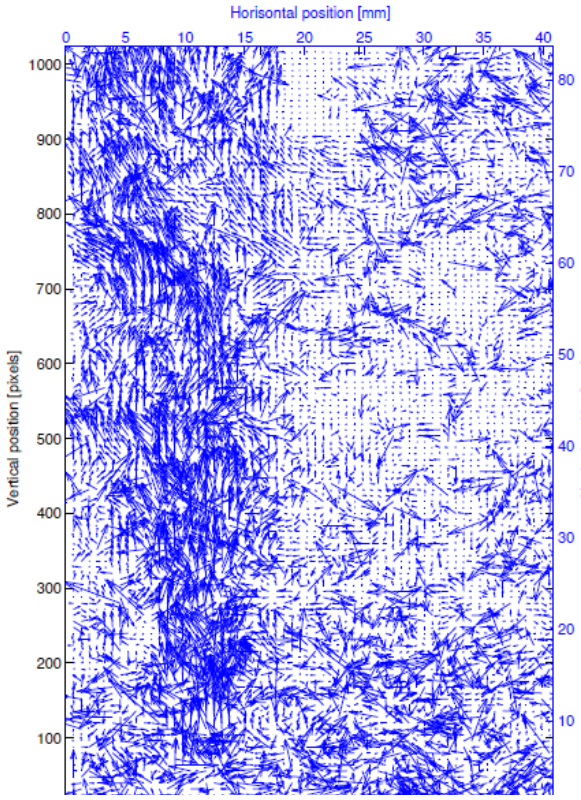

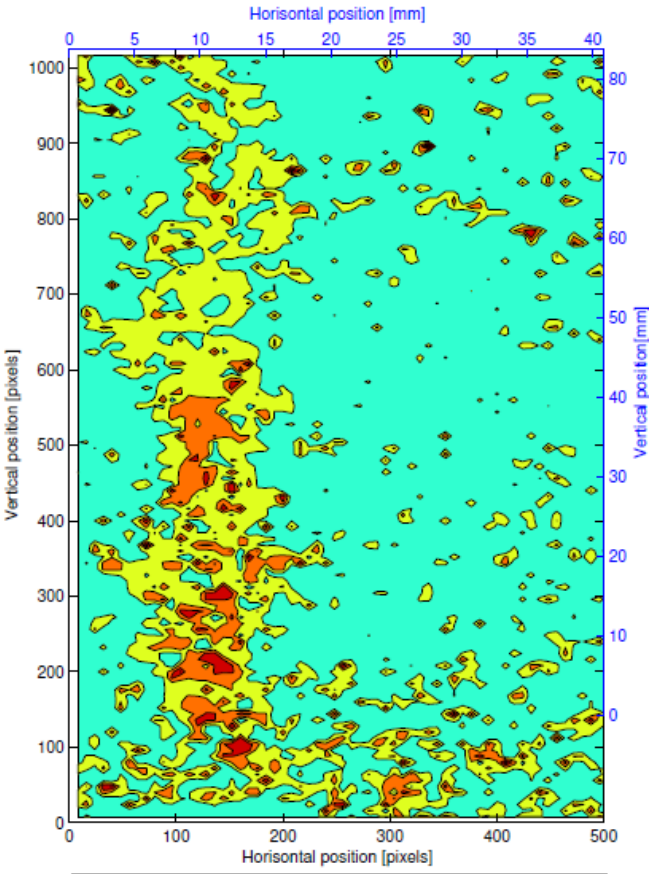

Figure 33: Velocity vector in non-Newtonian flow of 200 ppm PAC [33]

Figure 34: Velocity contours for the non-Newtonian flow [33]

The scale on Figure 34 ranges from 0 to 1200 which equals to velocity of -140 to 220 mm/s.

Herimonja A. Rabenjafimanantsoa together with Rune W. Time and Arild Saasen did experiments by applying UVP and PIV simultaneously. PIV is used for reference measurements for the UVP experiments. The main setup is in small pipes and the visualization captured by the two methods is helpful for investigating various flow structures such as vorticity, streamline and velocity magnitude. By applying the two methods simultaneously, the velocity profiles can be compared. Rabenjafimanantsoa, Time and Saasen published two papers;

1. *Simultaneous use of PIV and UVP to measure velocity profiles and turbulence in jet flow, 2006 [55].*
2. *Simultaneous UVP and PIV measurements related to bed dunes dynamics and turbulence structures in circular pipes, 2006 [35].*

5. Non-Invasive Measurements and Commercial Available Products

In the industry there are several systems available: intrusive, non-intrusive, active and passive methods. In this chapter the different commercial equipment will be discussed and reviewed for characterization purposes of liquid-particle flows.

Applying non-invasive methods opens possibilities such as retrofit to an existing plant without invasive costly removals or replacement of old and outdated equipment. Some of the main reasons for choosing non-invasive methods are to avoid high cost, scenarios of contamination, loss of expensive liquid, spill hazardous fluids and verification of flow performance [37]. Flow related non-invasive techniques can be divided into five categories (when ignoring temperature sensors):

1. Ultrasonic
2. Acoustic
3. Sonar
4. Nucleonic
5. ECT Tomography

The different techniques can be used together or as individual [37].

5.2 Ultrasonic devices

Ultrasonic devicess are mainly based on two methods: Ultrasonic flow meters and Pulse-echo units. The two units will be covered in the next chapter [37].

5.1.1 Ultrasonic flow meters

Ultrasonic flow meters (USFM) are the most common form of ultrasonic devices and are used in several industrial fields. The principle is emitting a beam of ultrasonic energy to the desired area from a transducer. A transducer is often used for both transmitting and emitting the signal traveling through the pipe and fluid. A sonic compound or gel are applied between the sensor and pipe to improve the transmission and reception of the signals and making the system more repeatable. To reduce the systematic errors due to positioning and mounting of the device, a mounting gauge or clamping bar is included so the transducer is located at the

proper position. If the system is to be installed permanent, they are often welded to the pipe. In order to operate the flow meter, the acoustic impedance of the transducer, coupler, pipe wall and fluid needs to be accounted for because the signals propagates differently in each material. The amount of signal and the angle of propagation are both critical units. The accuracy of these meters are optimal <1%, but in practice the general accuracy is +/- 3%. There are two main approaches to derive the flow rate; Time of Flight method (TOF) also known as Transit-Time method (TT) and the Doppler shift method [37].

The Transit-Time method is the most common method. Ultrasonic signal is emitted with an angle across the pipe. The flight time of the signal between the two transducers are connected to the flow velocity of the fluid and speed of sound in the fluid. Upstream measurements and downstream measurements are utilized by changing the first transducer from transmitter to receiver and opposite for the second transducer. This allows the fluid velocity to be calculated without including the sound speed if operating under constant conditions [37].

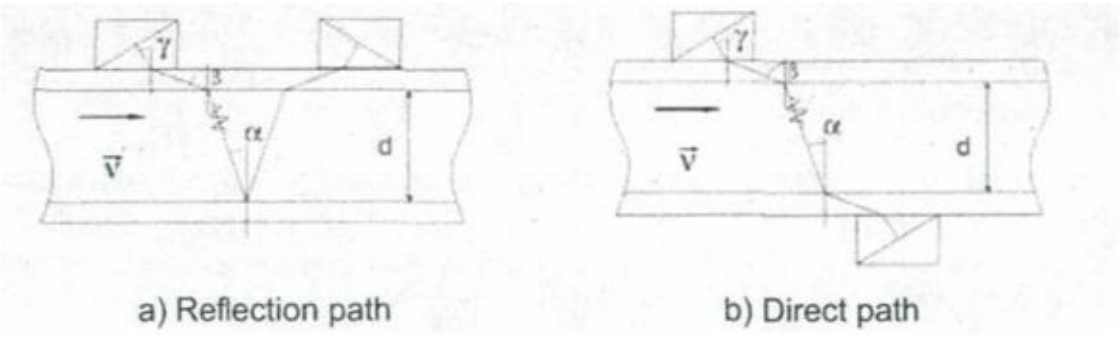

Figure 35: Basics of Transit-Time (TT) clamp-on [37]

Figure 35 shows the two different setups for the transducers. The left hand side illustration has the transducers mounted on the same side of the pipe, and the signal is reflected from the opposite wall between the two transducers. The "reflection" setup is most common in small diameter pipes. The right hand side illustration shows the "direct path" transducer setup and is applicable for pipes with larger diameter [37].

The flow velocity is an average value across the path and a Reynolds number based profile correction factor needs to be applied. Most manufacturers develop their own profile correction factor in order to determine whether flow is laminar or turbulent. Several producing companies of these systems result in varying profile correction factors and is a

source for variable measurement accuracy. If the derived sound speed corresponds to an expected value, the density of fluid and pipe diameter can be applied to calculate the mass flow. The simpler TT methods are not applicable for liquid-particle flow because the beam can be dispersed and attenuated. Enhancement in the software methods makes the method more suitable for fluid containing solid content. The largest area for false results is the transitional profile between laminar and turbulent flow [37].

The Doppler shift method is based on one transducer sending and receiving an ultrasonic beam. The emitted beam reflects on particles in the flow, and the frequency shift can be detected by the receiver. The frequency shift is related by a linear function to the flow velocity. In order for the signal to bounce of the particles, the flow needs to have a sufficient concentration of at least 25 ppm and particle size larger than 35 µm (for a 1 MHz beam). For lower frequencies the flow must have higher concentrations and larger particles. In Figure 36 a simple outline of the setup is shown.

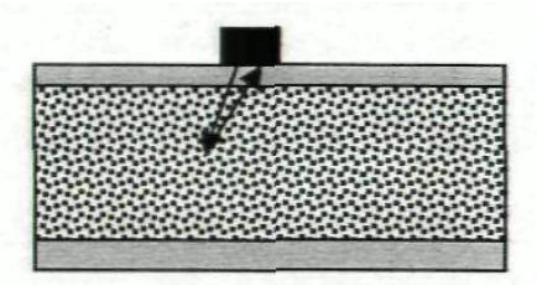

Figure 36: Doppler shift method [37]

The transducer operates as a transmitter and emitter of the ultrasonic energy as seen in Figure 36. This Doppler meters are very common in slurry handling industries and operates mostly between 1 and 2 MHz. The accuracy is limited to +/- 2% due to the uncertainty of which part of the flow is being measured [37].

5.1.2 Pulse Echo Method

Pulse Echo Method is the second type of ultrasonic device and is similar, but simpler than the clamp on USFM. The projected beam is directed right-angled to the pipe and the time delay of the reflected beam (echo) is measured. The method can be used to measure the interface level if the speed of sound for the fluid is known. Error in the reading will occur if the pipe is not completely full or empty.

5.2 Acoustics

Passive equipment records noise generated by the system and further relates the patterns or features to the frequency spectrum to the flow rate. Some systems use pressure reduction devices to listen to noise. By using pattern recognition techniques the various features can be detected.

Acoustic Emission (AE) is a very common technique in the Non-Destructive testing industry. A sample is exposed to external mechanical force and sensors are used to passively listen to frequencies of 10 KHz to 2 MHz. The exposure of an abrupt mechanical load or rapid pressure and temperature changes results in a short lived, high frequency elastic wave in the form of small material displacement or plastic deformation [37,38]. AE has also been applied in the process industry for measuring flow rate, leak detection and sand content. The method is effective for slurries containing hard particles. By knowing the flow rate in the system, the slurry mixture can be derived from particle impact signals. The sensors are mounted where the particles are most likely to collide with the pipe, and by cross-correlating signals from two detectors it would be possible to derive the flow rate.

5.3 Sonar methods

Sonar methods use passive sensors mounted along a pipe to characterize and interpret naturally occurring pressure fields. Features such as vortices and pressure ripple occurring in the pipe are commonly investigated by an array signal processing method. The technique is similar to underwater sonar navigation and therefor referred to as sonar. The frequency range of the method lies in the range of 100 to 1500 Hz and was introduced in the oil industry for multiphase measurements in 1998. The method is also applicable for single phase flows. Two forms of signal processing can be used to characterize features; Sonar based convective and Sonar based acoustics [39].

5.3.1 Sonar based convective

Sonar based convective is used to characterize the speed of coherent vortices or eddies flow past the array of sensors. The flow measurement can be done by using pressure sensor or strain based sensors. The coherent structure occurring in turbulent flow can be characterized

by applying a k-ω plot. The convection velocity of the coherent structures is computed by a sonar based algorithm and the volumetric flow rate can be determined. In Figure 37, the convective ridge is displayed using the k-ω plot [39].

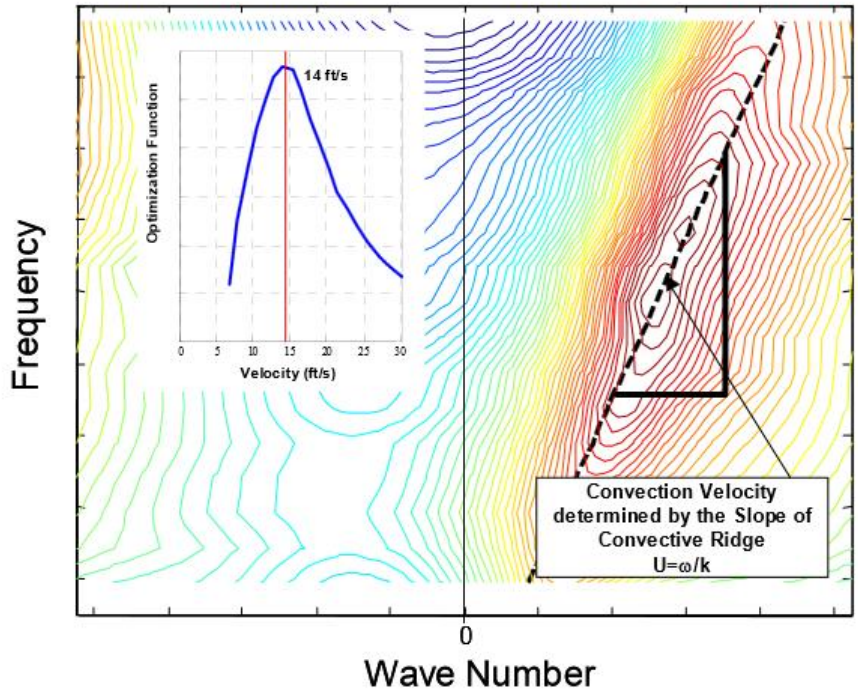

Figure 37: K-ω plot displaying convective ridge [39]

In Figure 37 the vertical axis is the temporal frequency [rad/sec] and given by

$$\omega = kU_{convect} \tag{38}$$

where $U_{convect}$ is the phase speed of the disturbance. The horizontal axis is the wave number [length^{-1}] and is given by

$$k = \frac{2\pi}{\lambda} \tag{39}$$

where λ is the wavelength. From the plot, the power associated with a pressure field convecting with the flow is distributed in regions that satisfy the dispersion relationship. This region is referred to as the convective ridge for turbulent flows, and the slope of the ridge on the plot indicated the speed of the turbulent eddies. By identifying the slope and applying correct calibration, the volumetric flow rate can be determined. According to Gysling and Loose (2003), the accuracy of this method is within +/- 0.5% in a wide operating range [39].

5.3.2 Sonar based acoustics

Sonar based acoustics is applicable for flow measurement based on comparison of ambient flow. The method use information from the convective pressure field associated with the convention of coherent structures. Another application is determining volumetric flow rate by characterizing acoustic pressure field. The same signal processing algorithm is used to create the k-ω plot, but in this case to identify acoustic ridges for the sound travelling with and against flow direction. The gradient to the ridges in Figure 38 is used to derive speed of sound and volume flow velocity [39,40].

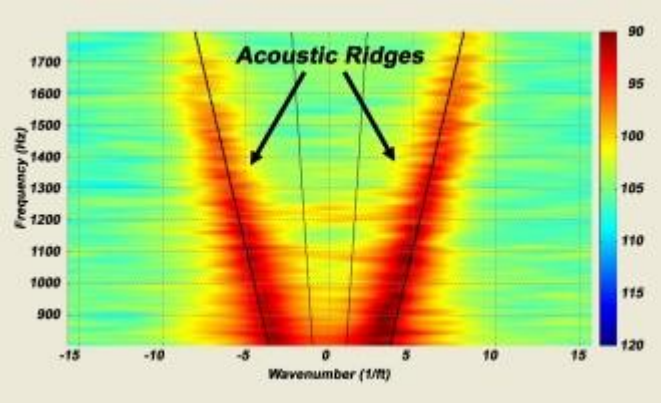

Figure 38: k-ω plot with acoustic ridges [40]

This method is applicable when the ratio of mixture flow rate to speed of sound (often referred to as Mach number) is of non-neglectable values. Since no reference data was obtained by Gysling and Loose (2003) there are no accuracy statement [39].

5.4 Nucleonic Methods

Nucleonic methods are based on the principle of using radioactive or gamma ray sensors to emit and detect changes in density of the material. The normal setup is by mounting sensors on opposite sides of the pipe. The relationship of density and intensity is obtained during the calibration with known factors as pipe wall thickness and reference fluid. The technique is highly dependent on reference fluid, so if the fluid properties change, the system need to be re-calibrated [37].

5.5 Tomography

Tomography is quite different from the non-invasive technique mentioned above. The principle is to provide information by an image, a tomogram, of the spatial distribution of the pipe content. Series of sensors are set along the pipe. Then, a signal is applied to each sensor in turn and monitoring the received signal at all of the other sensors. The result is a series of slices at different positions along a pipe. After the scanning is complete the data is processed and a tomogram can be created. A typical set of sensors are 8 or 16 and the resolution increases with numbers of sensors and complexity of the processing algorithm that is used.

Tomography is commonly used in the industry for multiphase flow related measurements. Tomograpy is therefore often referred to as "Industrial Process Tomography". There is a number of physical properties that can be measured with tomography and each technique has their parameter included in the name. The most relevant techniques for this thesis are Electrical Capacitance Tomography (ECT), Electrical Resistance Tomography (ERT) and Electromagnetic Tomography (EMT). In order for ECT, ERT and EMT to work properly, the fluid that is investigated need to be dielectric. If the pipe walls are conducting, the sensors must be wetted and electrically isolated from the pipe [37].

To get a general overview of the area of application, a table with each non-invasive method is seen in Table 2.

Table 2: Summary of Non-invasive methods and area of application [37]

Technology		USFM	Pulse-echo	Sonar	Nucleonic	Acoustic	ECT Tomography
Measured Parameter	Averaged flow	x		x	x (Vertical)	x	x
	Speed of sound	x		x			
	Density				x		
	Solids content					x	
	Wall thickness		x				
	Flow pattern						x
	Zoned flow						x
Applicable fluids	Liquid	xxxx	x	x	x	x	
	Sand/ oil					x	
	Gas	xx	x	x			
	Wet gas		x	x		x	
	Two phase		x		x		x
	Multiphase		x		xxxx	x	x

5.6 Ultrasonic Commercial Meters for Liquid

Several meters are available on the market. In this thesis the most relevant will be mentioned; Krohne, Endress+Hauser and Siemens.

5.6.1 Krohne UFM 610P and Optisonic 6300

The Two clamp-on flow meters from Krohne is operated by the transit time principle with one transducer pair. The UFC 610P is a portable device for measuring volumetric flow rate and volume flow with particles less than 1 %. The error in measurement is less than 2% [41]. The Optisonic 6300 use one UFC 300 signal converter and is used to obtain continuous measurements of volume flow, mass flow, flow speed, velocity of sound, SNR and values for diagnose purposes. The system operates with pipe sizes from 50-4000 mm [42].

5.6.2 Endress+Hauser's Prosonic Flow Meters

Endress+Hauser delivers six ultrasonic systems for flow measurements designed for Oil and Gas industry. The systems are available for miniature pipes and pipe size diameters up to 3000 mm as well for extended temperature ranges. The first Krohne flow meter was introduced for the Petroleum industry in 1997 and they rapidly became the world's leader in the field of ultrasonic in-line flow meters. Accessories such as pipe wall thickness sensor, in cases where corrosion environment are present and sensors for velocity of sound measurement system for unknown liquids are available [59].

5.6.3 Siemens Sitrans FUS1010 Meter

Siemens delivers their flow meters with the "Widebeam" technology which uses transit time or Doppler mode. The wider beam is claimed to be advantage if changes in fluid sonic velocities occur and is more tolerant of entrained solid in the flow. A thickness gauge can be mounted together with the sensors to achieve best results. Accuracy is stated to vary in the range of 0.5 to 1%, given the flow velocity is greater than 0.3 m/s [60].

5.7 Acoustic Commercial Sensors

Two manufacturers are described in this chapter. ClampOn is the largest supplier of acoustic systems compared to the second manufacturer, Abbon, who started up in 2004.

5.7.1 ClampOn DSP Particle monitor & ClampOn SandQ Monitor

Since ClampOn started up in 1995 it has grown to be the largest supplier of passive ultrasonic systems for sand and particle monitoring in the oil and gas industry. More than 6500 sand monitor systems are delivered to operators all over the world. ClampOn delivers basically three different products that operate either topside or subsea with active and passive acoustics;

SandQ Monitor is used for topside measurements and is based on passive and active acoustics. The mixed flow velocity is measured by a sensor installed a few diameters downstream of a bend in preferably turbulent flow. The passive acoustics measures sand and particles by detecting collisions as the particles impact the pipe wall. The sensor is located just after the bend for best results. The product flow is measured by an active Pulse-Doppler technique and the particles are tracked with an updating pulse of 8000 pings/s. The sensors are applicable for both single phase and multiphase flow and since the pulse rate is so high, the trend of the flow is very accurate. A digital signal processing unit also referred to as DSP registers unrelated noise from flow and chokes which is analyzed by filters. This unit replaces any analogue filters, circuits and amplifiers and the sensors can operate in several ultrasonic frequency ranges at the same time. All signal processing is done internally by the unit before the results are sent to the control system, hence no calculating interface is needed. The most important feature with the system is that operation parameters can be reviewed in real-time for optimizing the production by a two-way communication with the sensors and the control system [31].

There are always some restrictions when measuring flow under varying reservoir/well conditions, where temperature, pressure, fluid fractions etc. are continuously changing. With the factory calibrated system the uncertainty for sand is +/- 5% and +/- 15% for the flow. The range of measurable velocity is >0.5 m/s for sand and 0.15 to 15 m/s for flow. Minimum particle size for detection is 25 µm in oil and 15 µm in gas. Figure 39 shows how the system in mounted on a production pipe [31].

Figure 39: ClampOn SandQ Particle detector [31]

DSP-06 Particle Monitor is designed for topside and is quite similar to the SandQ described above. The main difference is that the DSP-06 is based on passive acoustics and an intelligent sensor only. The sensor is mounted two pipe diameters after a bend, just as the SandQ. The patented intelligent sensor records the collisions. The DSP engine and filter will process the readings and transfer the results to the control system. Real-time monitoring is available and a new filtering technique makes it a handy tool for analyzing sand production for optimized production. Figure 40 is a picture of the system, the dimension of the instrument is 101 x 211 mm [31].

Figure 40: ClampOn DSP-06 Particle detector [31]

The DSP-06 Subsea Model is applicable for deep water where high pressure environments occur. The intelligent sensor and DSP unit sends information topside to the control system. The subsea model is based on the same principle as the topside model, where the sensor is connected to the pipe after a bend. By scanning through a frequency range of 1 MHz 128 times per second and applying noise filtering, a good signal to noise ratio can be obtained and good indications of sand production can be monitored. One of the benefits of using subsea sensors is early notification of sand production and the signals are experienced to be stronger than on a topside sensor. When producing from a conventional well with topside sensors, the notification of producing sand will not arrive before the sand has arrived in the topside facilities. With the Subsea sensor, sand production will be notified immediately after flow has passed through the subsea tree. The result is a reduced chance of filling the process equipment with sand by early notification. A good example when subsea systems are useful is when producing from multiple wells in sidetracks or bypasses. If the sensor is located topside it will be difficult to know which well that has started to produce sand. With the subsea application this will not be an issue [31].

The downside of using subsea sensors is if the system fails or need service. This can be quite costly and would not be a preferred scenario for the operator. ClampOn's system for deep sea application is equipped with diagnostic features with intelligent health test of electronic hardware in form of two-way communication. The two-way communication makes it possible to upgrade to new software as well. Figure 41 show how the system is connected to the production pipe [31].

Figure 41: ClampOn Subsea DSP-06 [31]

5.7.2 Abbon Flow Master

The Flow Master is based on advanced software processing software of passive acoustic energy patterns measured at a single clamp-on sensor. The sensors are mounted to a choke valve or another component that will generate flow noise. The characteristics of the flow rate and composition of the flow is determined from the acoustic energy generated from the valve. The technology is sufficient to acquire information such as multiphase flow measurements, wet-gas measurements, sand detection, slug flow analysis and foam detection. The accuracy is claimed to be less than 1%, depending on the calibration method. The system is either calibrated in the test facility or on site [37].

5.8 Sonar Commercial Systems

Both Expro and Cindra delivers sonar based clamp-on meters. Cindra was the first to introduce sonar systems for flow characterization in 2003 [37].

5.8.1 Cindra SONARtrack® VF-100

The VF-100 is based on passive sonar and is used for both clear liquid and abrasive slurry. The system is designed for down hole demanding offshore environment and method for measurement is convection, which is described in *chapter 5.3.1 Sonar based convective.* Each sensor is clamped on the pipe section of 50.8 to 914.4 mm nominal bore and a processing technique measures the rate of turbulent eddies that convect past the sensor array. These turbulent structures were described in detail in *chapter 1.3.* The system measures volume flow with accuracy of +/- 1% within the range of 1-10 m/s [37,43].

5.8.2 Expro SonarMonitor™

Expro delivers both active and passive clamp-on sonar. The active flow meter uses a pulsed-array sensor to track the speed of the structure in the flow. The result is enhanced SNR and is more appropriate for low flow rates and thick pipe walls. The passive system is suggested for flow with higher rate and high liquid loading, and is similar to the Cindra SONARtrack® described above. Both the passive and active systems are relevant for single and multiphase flow [44].

5.9 Nucleonic Commercial Devices

Two nucleonic devices are investigated in this section; The Tracerco™ Density Gauge Type PRI 121/116 and Aker Solution's DUET multiphase meter [37].

5.9.1 Tracerco™ Density Gauge Type PRI 121/116

The clamp-on density gauge is designed to deliver reliable density values in oil and gas production process. The radioactive source Caesium-137 provides information such as density in single and multiphase, measurement of oil-in-water or water-in-oil and indications of solids build-up. The accuracy depends on the strength of radiation field at the detector and the selected response time [45]. This and all of the γ-densitometers needs to be calibrated for known fluids in order to measure absolute density levels, rather than simple density changes [37].

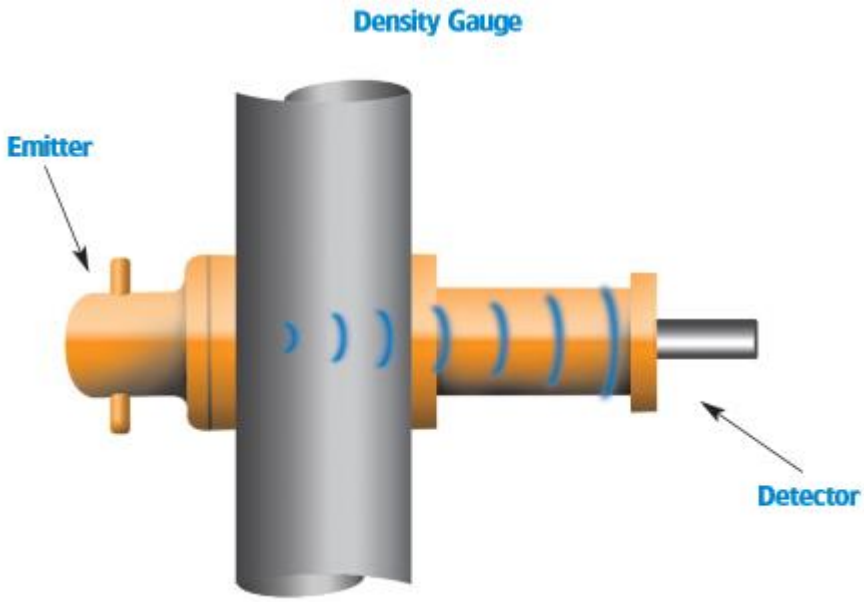

Figure 42: Tracerco™ Density Gauge PRI 121/116 [45]

5.9.2 Aker Solution's DUET Multiphase meter

The Duet multiphase flow meter is designed for topside and subsea application, and utilize a combination of dual energy gamma ray transmission and cross-correlation, hence the name DUET [46]. The result is simultaneous measurement of flow rates of several phases that occupies the pipe. The system was developed by CSIRO in 1997 and use Ceasium-137 and Americium-241 gamma ray densitometers. The system can replace expensive subsea test

lines or topside well test separators. The accuracy for liquid flow rate is +/- 10 % and <4 % for water-cut [37].

5.10 Tomographic Commercial Systems

Two systems will be regarded in this section: The TomoFlow R100 and Industrial Tomography system (ITS) p2000 and m3000. Some of the systems are based on combining ERT and ECT, hence referred to as dual-modality systems [37].

5.10.1 TomoFlow R100

The TomoFlow R100 use electrical capacitance tomography principle which is described in *chapter 5.5 Tomography*. 6, 8 or 12 senor electrodes are set up for tomography with cross-correlation and pattern recognition techniques for view of fluid/solid mixture and flow rate across the pipe section. Off-line multiphase flow analysis software "Flowan" is also available for calculations of detailed statistics and flow patterns [37] [47].

5.10.2 ITS p2000 and m3000

The p2000 is based on ERT, while the m3000 is a dual system with ERT and ECT. Both are available in two sizes; compact for one or two planes and full size for eight planes [37]. The m3000 was successfully applied for multiphase flows by Polimeri Europa, a company wholly owned subsidiary of Eni [48].

6. Discussion and Conclusion

To get a basic understanding of the aspects of liquid-particles that can occur when drilling mud returns while circulating the well, several established theories within slurry have been studied. Some of the important aspects are particle support mechanisms, transportation by suspended particles, flow patterns, impact of inclination vs horizontal wells, critical velocities and depositional velocities.

During a drilling operation the drilling mud should be designed to carry cuttings through the annulus to ensure a cuttings free borehole. non-Newtonian fluids are the common choice based on their superior properties compared to Newtonian liquids. Different studies such as Rabenjafimanantsoa et al. (2005) [54] compares water and PAC in terms of particle transport over dunes including pressure drop and transport velocity. This coincides with conclusion by Ramadan (2005)*;*

> Experimental and modeling studies suggested that, in addition to the flow rate, the rheology determines cutting transport capacity of drilling fluids. non-Newtonian fluid properties such as shear-thinning and thixotropic behaviors (yield stress) are normally considered in selecting a drilling fluid that has higher cutting transport ability with optimum frictional pressure loss [7].

A automatic cuttings circulation system was described with various systems for determining viscosity, density, particle size distribution, total cuttings weight and cuttings mineralogy. The methods were briefly described and ultrasonic methods such as USFM and UE are some of the alternative methods that can be included in a system for measuring flow velocity, particle size distribution, viscosity and density.

A problem by applying ultrasonic flow meters to conditions including particles, are interruptions by sediments accumulating in one part of the flow, such as horizontal flows with low velocities. The results can then be dominated by strong signals from the particles and velocity will reflect the particle velocity instead of liquid velocity. An Ultrasonic Extinction system should be considered for such a system of automatic drilling monitoring. The PSD tool is applicable for Off-line, In-line and On-line measurements of volumetric

solids concentration. The limitations and advantages for using such a system was reviewed in Table 1.

To identify and characterize liquid particle flow a literature study of acoustic and ultrasonic measurements was done and proved successful in several studies. Detection of oversized particles was the main area of acoustic measurements and the principle is used in state-of- art technology by ClampOn. Velocity measurements and attenuation measurements were the main focus of investigation in ultrasonic measurements. Utilizing attenuation measurements are used to reveal particle size or inter-particle distance. Regarding the acoustic attenuation, several theories exists. The earlier theories of Epstein, Carhart, Allagra and Hawley were reviewed by Dukhin and Goetz (2002) and resulted in a more accurate model. The main problem was that the earlier studies of ECAH did not account for particle-particle interaction, which was argued for by Dukhin and Goetz (2002) [30]. Velocity measurements such as PIV and UPV proved valuable for obtaining velocity profile, particle velocity suspended in a liquid and a two-dimensional, with two-or-three component velocity vector field. The application of these two methods has also used simultaneously by Rabenjafimanantsoa et al. (2006a) [55] and Rabenjafimanantsoa et al. (2006b) [35].

A complete solution for characterizing liquid-particle flow is not presented in this thesis. That would take a lot more than a master's thesis and rather extensive field experiments and testing. By learning the theories describing the impact of these suspensions give a wider knowledge on what parameters needs to be accounted for. A complex measurement method is useless if the theory supporting it is wrong. In *chapter 1* some important parameters were mentioned since they are characterizing the flow. These are: particle size, solid concentrations, flow pattern, particle and slurry velocity, turbulence and pressure drop.

In the last section of the thesis, relevant non-intrusive methods such as Ultrasonic, Acoustic, Sonar, Nucleonic and ECT Tomography are described. In Table 2 each method is summarized with measureable parameter and environments where the system can be used. State-of-art technology is included with accuracies for various environments are also mentioned. The Sonar method is one of the systems that use turbulent structures such as eddies to obtain flow measurements non-invasively. By measuring the velocity of the coherent structure and applying Reynolds number correlations, the volumetric flow rate is obtained.

An alternative would be to simultaneously use non-invasive methods of measurements, and not only use ultrasonic and acoustic. This is because every type of system has their strengths and weaknesses. In environments where ultrasonic sensors give false results, alternative methods such as Sonar or Nucleonic methods can give more reliable results.

The application of ultrasonic and acoustic systems for characterization of liquid-particle flow is not widely used, even though they are extremely versatile for such a purpose. The lack of a field proven hole cleaning monitor system gives huge opportunities. The field of ultrasound and acoustic needs to be further developed and field tested in order to convince operators in the petroleum industry that this is a reliable technology for hole cleaning monitoring.

Literature

[1-60]

1. Crowe CT. Multiphase flow handbook. Boca Raton, Fla: CRC/Taylor & Francis; 2006.

2. Albion K, Briens L, Briens C, Berruti F. Multiphase Flow Measurement Techniques for Slurry Transport. International Journal of Chemical Reactor Engineering. 2011;9(1):18-19.

3. Rabenjafimanantsoa HA. Particle transport and dynamics in turbulent Newtonian and non-Newtonian fluids [PhD. Dissertation]. University of Stavanger, Norway; 2007.

4. Statoil. Transport of produced sand [Web]. 2011. Cited 28.05.2014 Available from: http://www.statoil.com/en/TechnologyInnovation/FieldDevelopment/FlowAssurance/Pages/TransportOfProducedSand.aspx.

5. Doron P, Barnea D. Pressure drop and limit deposit velocity for solid-liquid flow in pipes. Chemical Engineering Science. 1995;50(10):1595-1604.

6. Doron P, Simkhis M, Barnea D. Flow of solid-liquid mixtures in inclined pipes. International Journal of Multiphase Flow. 1997;23(2):313-323.

7. Ramadan A, Skalle P, Saasen A. Application of a three-layer modeling approach for solids transport in horizontal and inclined channels. Chemical Engineering Science. 2005;60(10):2557-2570.

8. Duan M, Miska SZ, Yu M, Takach NE, Ahmed RM, Zettner CM. Transport of Small Cuttings in Extended-Reach Drilling. Paper SPE 103192 presented at the SPE international Oil and Gas Conference and Exhibition, China, 5-7 December 2008.

9. Petrowiki. Hole Cleaning [Web]. PetroWiki; 2013. Cited 28.05.2014. Available from: http://petrowiki.spe.org/Hole_cleaning.

10. Peker SM, Helvaci SS. Solid-Liquid Two Phase Flow. Oxford: Elsevier Science; 2011.

11. Hussain A. Role of coherent structures in turbulent shear flows. Proceedings of the Indian Academy of Sciences Section C: Engineering Sciences. 1981;4(2):129-175.

12. Hussain A. Coherent structures and turbulence. Journal of Fluid Mechanics. 1986;173:303-356.

13. Sechet P, Le Guennec B. The role of near wall turbulent structures on sediment transport. Water Research. 1999;33(17):3646-3656.

14. Matousek V. Pressure drops and flow patterns in sand-mixture pipes. Experimental Thermal and Fluid Science. 2002;26(6–7):693-702.

15. Britannica E. Ultrasonics [Web]. 2014. Cited 04.06.2014. Available from: http://www.britannica.com/EBchecked/topic/613488/ultrasonics.

16. Byu. What is Acoustics? [Web]. 2013. Cited 04.06.2014. Available from: http://www.physics.byu.edu/research/acoustics/what_is_acoustics.aspx.

17. Asaa. Acoustical Society of America Awards [Web]. Cited 04.06.2014. Available from: http://asa.aip.org/awards.html.

18. Albion K, Briens L, Briens C, Berruti F. Modelling of oversized material flow through a horizontal hydrotransport slurry pipe to optimize its acoustic detection. Powder Technology. 2009;194(1–2):18-32.

19. Wrobel BM. Measurement and Characterization of Liquid-Particle Flow [PhD. Dissertation]. University of Stavanger, Stavanger 2012.

20. Britannica E. Tansducers [Web]. Encyclopædia Britannica Inc; 2014. Cited 04.06.2014. Available from: http://www.britannica.com/EBchecked/topic/613488/ultrasonics.

21. Ndt. Non-destructive tesing [Web]. Cited 04.06.2014. Available from: http://www.ndt-ed.org/EducationResources/CommunityCollege/Ultrasonics/cc_ut_index.htm.

22. Urick RJ. A Sound Velocity Method for Determining the Compressibility of Finely Divided Substances. Journal of Applied Physics. 1947;18:983-987.

23. Ament WS. Toward a Theory of Reflection by a Rough Surface. Proceedings of the institute of Radio Engineers IRE. 1953;25:638.

24. Stolojanu V, Prakash A. Characterization of slurry systems by ultrasonic techniques. Chemical Engineering Journal. 2001;84:215-222.

25. Zwietering TN. Suspending of solid particles in liquid by agitators. Chemical Engineering Science. 1957;8:244.

26. Harker AH, Temple JaG. Velocity and attenuation of ultrasound in suspensions of particles in fluids. Journal of Physics D: Applied Physics. 1987;21:1576-1588.

27. Atkinson CM, Kytomaa HK. Acoustic wave speed and attenuation on suspensions. International Journal of Multiphase Flow. 1992;18(4):577-592.

28. Epstein PS, Carhart RR. The absorption of sound in suspensions and emulsions Applied Mechanics. Journal of the Acoustical Society of America. 1953;25(3):553-565.

29. Stakutis VJ, Morse RW, Dill M, Beyer RT. Attenuation of ultrasound in aqueous suspensions. Journal of the Acoustical Society of America. 1955;27:539–546.

30. Dukhin AS, Goetz PJ. Ultrasound for Characterizing Colloids Particle Sizing, Zeta Potential Rheology. Amsterdam, NLD: Elsevier Science & Technology; 2002.

31. Clampon. Topside and subsea ultrasonic intelligent sensors [Web]. Cited 04.06.2014. Available from: http://www.clampon.com.

32. Takeda Y. Velocity profile measurement by ultrasonic doppler method. Experimental Thermal and Fluid Science. 1995;10(4):444-453.

33. Rabenjafimanantsoa HA, Time RW, Hana M, Saasen A. Dunes dynamics and turbulence structures over particles bed Experimental studies and CFD simulations. Annual transaction of the nordic rheology society. 2005;13:171-176.

34. Mavros P. Flow Visualization in Stirred Vessels: A Review of Experimental Techniques. Chemical Engineering Research and Design. 2001;79(2):113-127.

35. Rabenjafimanantsoa AH, Time RW, Saasen A. Simultaneous UVP and PIV measurements related to bed dunes dynamics and turbulence structures in circular pipes. 5th International Symposium on Ultrasonic Doppler Methods for Fluid Mechanics and Fluid Engineering. 2007:63-67.

36. Weirich JB, Bland RG, Smith WW, Krueger V, Harrell JW, Nasr HN, et al., Drilling systems with sensors for determining properties of drilling fluid downhole. 2001, Google Patents.

37. Whitson RJ, Stobie GJ. An overview of Non-invasive flow measurements methods. The Americas workshop 3-5 February. 2009.

38. Asnt. Introduction to Nondestructive Testing [Web]. Cited 04.06.2014. Available from: https://www.asnt.org/MinorSiteSections/AboutASNT/Intro-to-NDT.aspx#AE.

39. Gysling DL, Loose DH. Sonar-based, clamp-on flow meter for gas and liquid applications. Presented at ISA 2004 Exhibit and Conference, Edmonton, Canada, April 2004.

40. Krohne. Passive sonar flowmeter technology: operating principles [Web]. Cited 04.06.2014. Available from: http://www.processonline.com.au/articles/32245-Passive-sonar-flowmeter-technology-operating-principles.

41. Krohne. UFM 610P [Web]. Cited 04.06.2014. Available from: http://www.krohne-downloadcenter.com/dlc/TD_UFM600T_610P_e_72.pdf.

42. Krohne. Optisonic 6300 [Web]. Cited 04.06.2014. Available from: http://www.krohne-downloadcenter.com/dlc/TD_OPTISONIC6300_en_090818_4000255303_R05.pdf.

43. Cindra. SONARtrac® Volumetric Flow Monitoring System [Web]. Cited 04.06.2014. Available from: http://www.cidra.com/sites/default/files/document_library/BI0012_VF100_Data_Sheet.pdf.

44. Expro. SonarMonitor™ Clamp-on Metering for Permanent Flow Measurement [Web]. Cited 04.06.2014. Available from: http://www.exprometers.com/Permanent_Clamp_on_Metering/.

45. Tracerco. TRACERCO™ Density Gauge Measurement in the Process Industry [Web]. Cited 04.06.2014. Available from: http://www.tracerco.com/pdfs-uploaded/US%20Tracerco%20Density%20Gauge.pdf.

46. Solutions A. DUET multiphase flow meter [Web]. 2002. Cited 04.06.2014. Available from: http://www.rigzone.com/news/article.asp?a_id=2746.

47. Tomoflow. R100 [Web]. Cited 04.06.2014. Available from: http://www.tomoflow.com/pdf/TFLR100spec.pdf.

48. Its. See inside your process [Web]. Cited 04.06.2014. Available from: http://www.kenelec.com.au/sitebuilder/products/files/902/itsflowapplications.pdf.

49. Saasen A, Omland TH, Ekrene S, Brévière J, Villard E, Kaageson-Loe N, et al. Automatic Measurement of Drilling Fluid and Drill-Cuttings Properties. Paper SPE 112687 presented at the IADC/SPE Drilling Conference, Orlando, Florida, 4-6 March 2009. 611-625.

50. Naegel M, Pradie E, Delahaye T, Mabile C, Roussiaux G. Cuttings Flow Meters Monitor Hole Cleaning in Extended Reach Wells. Paper SPE 50677 presented at the European Petroleum Conference, Hauge, Netherlands 20-22 October 1998. 611-612.

51. Omland TH, Saasen A, Taugbol K, Jorgensen T, Reinholt F, Amundsen PA, et al. Improved Drilling Process Control Through Continuous Particle and Cuttings Monitoring. Paper SPE 107547 presented at the SPE Digital Energy Conference and Exhibition, Housten, Texas, 11-12 April 2007.

52. Karimi M. Drill-Cuttings Analysis for Real-Time Problem Diagnosis and Drilling Performance Optimization. Paper SPE 165919 presented at the Asia Pacific Oil & Gas Conference, Jakarta, Indonesia, 22-24 October 2013.

53. Brown NP, Heywood NI. Slurry Handling: Design of Solid-liquid Systems. Essex, England: Elsevier Science; 1991.

54. Rabenjafimanantsoa HA, Time RW, Saasen A. Flow regimes over particle beds Experimental studies of particle transport in horizontal pipes. Annual transaction of the nordic rheology society. 2005;13:99-106.

55. Rabenjafimanantsoa HA, Time RW, Saasen A. Simultaneous use of PIV and UVP to measure velocity profiles and turbulence in jet flow. Annual transaction of the nordic rheology society. 2006;14:149-157.

56. Petrowiki. Pseudoplastic friction factor vs. Reynolds number [Web]. 2013. Cited 04.06.2014. Available from: http://petrowiki.org/Fluid_friction.

57. Ramadan A, Skalle P, Johansen ST, Svein J, Saasen A. Mechanistic model for cuttings removal from solid bed in inclined channels. Journal of Petroleum Science and Engineering. 2001;30(3–4):129-141.

58. Wikipedia. Moody diagram [Web]. 2014. Cited 07.06.2014. Available from: http://en.wikipedia.org/wiki/Moody_chart.

59. Endress. Flow meter measurements [Web]. Cited 10.06.2014. Available from: http://www.endress.com/en/products/flow.

60. Siemens. Sitrans FUS1010 flow meter [Web]. Cited 10.06.2014. Available from: http://www.automation.siemens.com/mcms/sensor-systems/en/process-instrumentation/flow-measurement/ultrasonic-flow-meter/clamp-on-flow/configurable-systems/pages/sitrans-fus1010-standard.aspx.